IN VIVO AND *IN VITRO* ANALYSES OF mRNA EXPRESSION OF ROBO2 IN ZEBRAFISH IN THE CONTEXT OF PI3K/AKT/TOR PATHWAY

A THESIS SUBMITTED TO
THE DEPARTMENT OF MOLECULAR BIOLOGY AND GENETICS AND
THE INSTITUTE OF ENGINEERING AND SCIENCE OF
BILKENT UNIVERSITY
IN PARTIAL FULFILMENT OF THE REQUIREMENTS FOR THE DEGREE
OF MASTER OF SCIENCE

BY
ERTUĞRUL DALKIÇ
AUGUST 2006

TO MY FAMILY

I certify that I read this thesis and that in my opinion it is fully adequate, in scope and in quality, as a thesis for the degree of Master of Science

_____

Asst. Prof. K. Can Akçalı

I certify that I read this thesis and that in my opinion it is fully adequate, in scope and in quality, as a thesis for the degree of Master of Science

_____

Dr. Sreeparna Banerjee

I certify that I read this thesis and that in my opinion it is fully adequate, in scope and in quality, as a thesis for the degree of Master of Science

_____

Asst. Prof. Özlen Konu

Approved for Institute of Engineering and Science.

_____

Director of Institute of Engineering and Science

Prof. Dr.

ABSTRACT

IN VIVO AND *IN VITRO* ANALYSES OF mRNA EXPRESSION OF ROBO2 IN ZEBRAFISH IN THE CONTEXT OF PI3K/AKT/TOR PATHWAY

Ertuğrul Dalkıç

M.Sc. in Molecular Biology and Genetics
Supervisor: Asst. Prof. Özlen KONU
August 2006, 81 pages

Robo2 is an axon guidance receptor, well-known for its repulsive role in the nervous system. In addition, Robo2 might regulate cell migration both during embryogenesis or in adulthood. In this study, a novel isoform of the zebrafish robo2 (robo2_tv2), which included an otherwise alternatively spliced exon (CAE), has been characterized. Robo2_tv2 was expressed differentially in most non-neuronal tissues of adult zebrafish whereas Robo2_tv1 expression to a great extent was restricted to the brain and eye. Our findings demonstrated that the amino acid sequence coded by CAE of the Robo2 gene was highly conserved between zebrafish and mammals, and also contained conserved motifs shared with Robo1 and Robo4 but not with Robo3. Furthermore, we provided an account of differential transcription of the CAE homolog in various tissues of the adult rat. These results has suggested that the alternatively spliced Robo2 isoforms may exhibit tissue specificity.

In addition, we investigated the transcriptional neighbors of Robo2 based on computational and experimental methods. Bioinformatics analysis of a published zebrafish microarray data by Mathavan et al. (2005) demonstrated that Robo2 expression might be correlated with a number of genes involved in the PI3K/AKT/GSK3B/TOR signaling; these genes included Rheb, Gsk3alpha, PP2A, and several Wnt signaling members. Analysis of a conserved coexpression network (Stuart et al. 2003) also placed Robo2 and Tor as indirect neighbors. Accordingly, several PI3K/AKT/GS3B/TOR signaling members, namely, Pik3r2, Akt2, Gsk3b were characterized in terms of their sequence conservation and tissue-specific expressions for the first time in zebrafish. Phylogenetic analysis has shown that these genes were moderately to highly conserved among different vertebrate taxa. RT-PCR and real-time RT-PCR analyses in various adult tissues and under specific growth-regulatory conditions (e.g., TOR inhibition, and serum starvation) suggested that Tor, Pi3kr2, Akt2 and Gsk3b mRNA might be regulated at the transcriptional level. However, these preliminary findings need to be further confirmed by using multiple independent experiments due to high variability and small fold changes that characterized the expression levels.

Future studies are planned to identify functional relevance for the alternative usage of CAE and determine how different isoforms respond to conditions that modulate cell growth/proliferation pathways involved in cellular stress conditions including cancer.

ÖZET

ZEBRABALIĞINDA ROBO2'NİN PI3K/AKT/TOR YOLĞIYLA İLİŞKİLİ OLARAK *IN VIVO* VE *IN VITRO* IFADE ANALİZİ

Ertuğrul Dalkıç

Master Tezi Moleküler Biyoloji ve Genetik
Tez Yöneticisi: Yard. Doç. Özlen KONU
Ağustos 2006, 81 sayfa

Robo2 sinir sisteminin önemli bir akson rehberliği reseptörüdür. Slit reseptörü olan bu protein, aksonların büyüme bölgelerinde itici bir görev üstlenir. Bunun yanında, normal hücre göçünde de rolü olduğu bilinmektedir. Bu çalışmada, zebrabalığında robo2 geninin yeni bir izoformu (robo2_tv2) bulunmuştur. Bu izoform alternatif olarak normalde kullanılmayan bir korunmuş alternatif egzonu (CAE) içermektedir. Robo2_tv2 farklı şekillerde sinirsel olmayan hücrelerde ifade edilirken, robo2_tv1 ifadesi göz ve beyin gibi sinirsel hücrelerle sınırlıdır. Bulgularımız CAE ye denk düşen amino asit sekansının zebrabalığı ve memeliler arasında önemli ölçüde korunduğunu göstermiştir. Ayrıca CAE amino asit sekansının robo1 ve robo4'te de korunduğunu bulduk. Zebrabalığının yanında sıçanda yaptığımız çalışmalar da alternatif CAE kullanımının değişik erişkin hayvan dokularında korunduğunu gösterdi. Bu sonuçlar, alternatif robo2 izoformlarının dokulara özel olarak kullanımını önermektedir.

Bunun yanında, robo2 geninin PI3K/AKT/TOR yolağı üyeleriyle olası bir yakınlığı deneysel ve bilgisayar destekli çalışmalar sonucu gösterilmiştir. Mathavan et al. (2005) mikroarray çalışmasının biyoinformatik analizi Robo2 nin PI3K/AKT/TOR yolağı üyeleriyle ilişkili olduğunu gösterdi. Bu genler arasında Rheb, Gsk3alpha, PP2A ve birçok Wnt sinyal yolağı üyesi yer aldı. Stuart el al. (2003) korunmuş birlikte ifade ağı analizi Robo2 ve Tor u indirekt komşu olarak gösterdi. Pik3r2, Akt2, Gsk3b genleri sekans ve ifade olarak analiz edildi ve zebrabalığında korunduğu gösterildi. Rapamycin verilmesi ve serum değerinin değiştirilmesi sonrasında bu ilginilen genlerin ifadeleri RT-PCR ve real-time RT-PCR metodlarıyla analiz edildi ve bu genlerin bahsi geçen koşullarda transkript olarak değişik ifadelerde bulunabileceği gösterildi ancak bu deneylerdeki örnek sayısı istatiksel olarak geçerli bir sonuca varmak için yeterli olmamıştır.

Gelecek çalışmalarda, alternatif CAE kullanımının fonksiyonel ilişkisi çalışılacaktır. Değişik robo2 izoformlarının değişik kondisyonlardaki davranışı kanser de dahil olmak üzere çalışılacaktır.

ACKNOWLEDGEMENTS

First of all, I would like to thank to Dr. Özlen Konu for her invaluable supervision during my study.

I would like to also thank to Dr. Can Akçalı and Iraz Aydın for their help with the rat study.

I would like to acknowledge TÜBİTAK for the graduate scholarship.

I would to thank my family for always supporting me.

I would like to thank Ceren, Koray, Cem and other current and previous Konu Lab Members for their help and friendship.

I would like to thank Ender, Şerif, Hani, Güvenç, Nuri, Bala and other MBG family members for their close friendship.

This project has been funded by a grant from TÜBİTAK (TBAG-2285 (103T038)) to Özlen Konu.

TABLE OF CONTENTS

LIST OF TABLES

LIST OF FIGURES

ABBREVIATIONS

APS	Ammonuim Persulphate
ATP	Adenosine triphosphate
AMP	Adenosine monophosphate
bp	Base Pairs
CAE	Conserved Alternative Exon
CHO	Chinese Hamster Ovary
DMSO	Dimethyl Sulfoxide
DNA	Deoxyribonucleic Acid
dpf	Days Post Fertilization
EDTA	Diaminoethane Tetra-acetic Acid
EGFR	Epidermal growth factor receptor
EtBr	Ethidium Bromide
hpf	Hours Post Fertilization
PAGE	Polyacrylamide Gel Electrophoresis
PBS	Phosphate Buffered Saline
PCR	Polymerase Chain Reaction
PDGFR	Platelet-derived growth factor receptor
PIP2	Phosphatidylinositol-4,5-bisphosphate
PIP3	Phosphatidylinositol-3,4,5-trisphosphate
RT	Room Temperature
RNase	Ribonuclease
TOR	Target of Rapamycin
Tris	Tris(Hydroxymethyl)-Methylamine
tv	Transcript variant
UV	Ultraviolet

CHAPTER I: INTRODUCTION

1.1. ZEBRAFISH AS A MODEL SYSTEM

Zebrafish is a well established model organism in the developmental biology field (Streisinger et al. 1981). There are several advantages of using zebrafish: First, it is a vertebrate, thus is evolutionarily closer to human when compared with invertebrate model organisms. This phylogenetic closeness enables researchers to highly relate the results of zebrafish studies to those performed on human biology and pathological conditions. In addition, zebrafish is easy to breed and handle in laboratory conditions; it reproduces in large numbers and externally; and has a relatively short developmental period. Another important characteristic of zebrafish is that the embryos are transparent, making the examination under light microscopy easy. Recent advances in sequencing and assembly of the zebrafish genome (Zv5, www.ensembl.org) also allow researchers to study evolutionary as well as functional relatedness of zebrafish genes to their human counterparts.

1.1.1. Zebrafish Development

The stages of zebrafish development have been studied extensively (Kimmel et al. 1995). A zygote period (0-3/4 hpf) is followed by a cleavage period (3/4-$2^{1/4}$ hpf), in which synchronous divisions of two blastomeres result in an embryo of 64-cells. Blastula period ($2^{1/4}$-$5^{1/4}$ hpf) is characterized by the formation of yolk syncytial layer, asynchronous divisions and cell rearrangements that lead to epiboly. Gastrula period ($5^{1/4}$-10 hpf) covers the formation of 50% epiboly to 100% tail bud structure; and segmentation period (10-24 hpf) is the stage somites are formed. In pharyngula period (24-48 hpf), embryo gains a body axis with somites, notochord and the brain. Finally hatching occurs between 48-72 hpf. Embryos are called larvae after hatching.

1.1.2 Zebrafish as a model for Human Disease

In addition to being a well established model for developmental biology studies, zebrafish also has been used to model human disease. In a recent study, a gene set significantly altered in zebrafish liver tumors was compared to gene sets from human tumors (Lam et al. 2005). Human homologs of zebrafish liver tumor gene set showed significant change in liver, gastric, prostate and lung tumor types, while the significance for liver was expectedly higher when compared with others (Lam et al. 2005). This high level of conservation was supported in another study that used an oncogenomic approach (Lam et al. 2006). Similarly, genomic structure, synteny, and the protein structures, i.e., important domains and highly mutated residues, of Fanconi Anemia genes also were shown to be conserved between humans and zebrafish (Titus et al. 2006). Another study showed that endocrine system of zebrafish was similar enough to that of human, indicating that whole system research could also benefit from the forward-reverse genetic techniques of zebrafish (McGonnell et al. 2006). These studies demonstrate the appropriateness of zebrafish as a model for human disease in addition to its well-known usage in development research.

1.1.3. Molecular and Genetic Studies Using Zebrafish Cell Cultures

Although, zebrafish is a powerful organism in many respects, zebrafish cell culture has not been used as widely as mammalian. On the other hand, zebrafish cell culture studies provide excellent possibilities to understand zebrafish gene structure, sequence, and function. First cell line from zebrafish was derived from one day old embryos, generating a fibroblast-like cell line (ZF4) (Driever et al. 1993). Usefullness of this new system was verified in a heat and cold shock experiment, as the change in *hsf1a* upon heat-shock was similar to that of zebrafish liver (Airaksinen et al. 2003). Suitability of zebrafish cell culture was confirmed in an innate immunity study in which ZF4 cells properly responded to zfIFN tranfection by plasmid (Altmann et al. 2004). Transfection capability of zebrafish cell lines was also exploited to analyze the response of cells to

alterations of zebrafish ATM (ataxia-telangiectasia mutated) in ZF4 (Garg et al. 2004). Not only embryo derived cell lines but also tissue-derived (e.g., liver, fin, etc.) cell lines were established for zebrafish. In a study in which the aryl hydrocarbon receptor (AHR) pathway in zebrafish liver cell line was investigated, the degradation of AHR in response to β-naphthoflavone and geldanamycin was shown to be conserved with mammals (Wentworth et al. 2004). Liver and caudal fin derived zebrafish cell lines were studied for their miRNA content and were shown to be similar to each other and also to adult male and female fish (Chen et al. 2005). In another study, the response of zebrafish metallothionein gene to several metal ions was tested both in zebrafish embryo-larvae and the liver cell line. *In vitro* induction of metallothionein gene was confirmed to be higher than that observed *in vivo* (Chan et al. 2006). These studies clearly demonstrate the usefulness of zebrafish cell culture systems for cloning and functional studies.

1.2. ROBO2 AS AN IMPORTANT REGULATOR OF AXON GUIDANCE AND CELL MIGRATION

1.2.1. Axonal Guidance Molecules and Robo-Slit Signaling

Axon guidance molecules govern the shaping of the nervous system. The interaction between the axon guidance cues and their receptors determine the direction of a growth cone of a neuron for its movement. Some ligand-receptor couples act as repellents and some are attractive, whereas a few could behave in either way depending on the cellular condition (Chilton et al. 2006). There exists a variety of axon guidance molecules such as Ephrins, Semaphorins, Netrins and Slits which may attract or repel a growth cone by the action of a guidance cue and its receptor (Chilton et al. 2006).

Robo (roundabout) is an axon guidance receptor that was identified in *Drosophila* as having a repulsive role in defining the axonal pathways of the central nervous system (Seeger et al. 1993). In *Drosophila*, axons of robo mutants form roundels because of repeated crossing and recrossing the midline instead of exhibiting well-defined axonal

paths (Seeger et al. 1993). Further studies indicated that Robo encodes a transmembrane membrane receptor protein that belongs to immunoglobulin superfamily (Kidd et al. 1998). Robo also has been shown to receive chemo-repulsive signals from Slit proteins to prevent inappropriate midline crossing (Kidd et al. 1999). Slit proteins are molecular guidance cues that were shown to guide neuronal and non-neuronal cell migration (Wong et al. 2002). Slit was identified as having a role in pattern formation; and it was shown to be required for embryonic central nervous system development of *Drosophila* (Nusslein-Volhard et al. 1984, Rothberg et al. 1988). Later, it has been demonstrated that there are two other homologs of Robo; Robo2 and Robo3, which also form complexes with Slit (Rajagopalan et al. 2000a; Simpson et al. 2000a; Rajagopalan et al. 2000b; Simpson et al. 2000b). Robo4, on the other hand, has been demonstrated to be an endothelial marker that was recently implicated as an angiogenic marker in colorectal cancers (Huminiecki et al. 2002, Grone et al. 2006). In summary, Slit and Robo family genes have roles in axon guidance and cell migration in mammals mostly in nervous system and in some non-neuronal tissues (Yuan et al. 1999, Marillat et al. 2002, Bagri et al. 2002, Long et al. 2004, Sundaresan et al. 2004).

1.2.2. Zebrafish Robo2 Protein

Robo function is conserved between zebrafish and mammals. Robo homologs have been cloned in zebrafish; and a full length cDNA sequence for Robo2 has been reported (Lee et al. 2001). Robo2 has been identified in zebrafish as ‘astray’, mutation of which prevented proper retinal axon guidance, anterior-posterior pathfinding, midline crossing, and fascicular retinal projection (Fricke et al. 2001). From the deduced aminoacid sequence, Robo2 has an extracellular domain comprising five immunoglobulin (Ig) domains and three fibronectin type III (FN) domains; a single transmembrane domain; and a cytoplasmic domain containing several conserved cytoplasmic motifs. Extracellular domain is highly conserved with other homologs wheras the intracellular domain has been shown to be divergent (Lee et al. 2001). The extracellular Ig domains allow the binding of Slit by its LRR (Leucine-Rich Repeat) and the intracellular part

determines the response of the cell to Slit signal (Chen et al. 2001, Battye et al. 2001, Nguyen Ba-Charvet et al. 2001, Liu et al. 2004).

1.2.3. Zebrafish Robo2 mRNA Expression Studies

Detailed analysis of the expression profiles of all three robo parologs during the first three days of zebrafish development indicated that Robo2 expression begins relatively later than the Robo1 and Robo3 mRNAs, at around 12 hpf in hindbrain (Lee et al. 2001). Expression of Robo2 increases over time and appears in various other regions of the nervous system in the embryo, becoming restricted to head at later stages. A significant characteristic of Robo2 is that its expression remains high at 72 hpf while the expression of Robo1 and Robo3 are diminished by that time. Robo4 expression in notochord begins at around 8 hpf while the vascular expression of Robo4 starts in angioblasts ventral to notochord at 19 or 20 somite stage and is lessened at 29 hpf (Bedell et al. 2005). It also has been shown that zebrafish Robo mRNAs are present in non-neural tissues in addition to neural tissues during the first 3 days of development. Robo2 has been shown to be expressed in pectoral fin buds at 32 hpf but is later turned off (Lee et al. 2001). Zebrafish Robo2 expression in nervous system supports the role of axon guidance which has been shown in another study (Fricke et al. 2001) and its expression in pectoral fin buds suggests a role in cell migration (Lee et al. 2001). Although Robo2 was shown to play an important role in axon guidance and cell migration during embryogenesis in zebrafish, its larval, juvenile and adult expression pattern or function in non-neuronal cells was not well-known.

1.2.4. Non-neuronal Expression and Function of Robo2

Several studies have reported the expression and role of Robo2 in non-neuronal tissues in chicken, rodents, and humans (Piper et al. 2000, Nagase et al. 2000, Vargesson et al. 2001, Anselmo et al. 2003, Greenberg et al. 2004, Grieshammer et al. 2004). The expression patterns of Slit family, Robo1 and Robo2 have been analyzed during murine metanephric development. Robo2 expression was shown in the induced metanephric

mesenchyme surrounding the arborizing urogenital tract tips and later in the proximal end of the S shaped bodies (Piper et al., 2000). The expression patterns of Slit family, Robo1 and Robo2 have also been analyzed during mouse limb development. (Vargesson et al., 2001). Slit and Robo family expressions have been analyzed during lung development; and it has been suggested that Robo1 and Robo2 have roles in branching morphogenesis and airway development (Anselmo et al., 2003). In a human study, Robo2 was designated as KIAA1568 and has been shown to be highly expressed in adult and fetal brain, adult ovary, and intermediately expressed in fetal liver and in adult lung, kidney, spleen, testis, and spinal cord, and scantily or not expresssed in adult pancreas, heart, liver, and skeletal muscle (Nagase et al. 2000).

1.2.5. Alternative Splicing Potential of Robo2

A common characteristic of immunoglobulin superfamily receptors is the frequent alternative splicing events they undergo (Brummendorf et al. 2001). There are several studies which unearthed evidence that proved tissue type dependent and in some cases neuronal/non-neuronal tissue distinct expression profiles of different isoforms of genes as a result of alternative splicing events (Fukuda et al. 2003, Shen et al. 2002, Jin et al. 2002, Rahman et al. 2002, Ramming et al. 2000, Hu et al. 1999). One study clarified different isoforms of Neogenin1, also an axon guidance receptor in zebrafish, with tissue specific expression patterns (Shen et al. 2002). Another study identified a neuronal- or non-neuronal expression of different isoforms of FE65, a neuronal adaptor protein (Hu et al. 1999). Robos are also members of immunoglobulin superfamily receptors. Previously, Robo1 and Rig1 members of Robo family have been shown to possess different isoforms that are generated by alternative splicing (Clark et al. 2002, Yuan et al. 1999). Rig1 has several alternatively spliced exons that were implicated in the generation of different isoforms of Rig1, defined as the transmembrane and the secreted forms, each with distinct functions (Yuan et al. 1999). In another study, alternative splicing of Robo1 in mouse has been shown to generate two different isoforms, namely, Robo1 and Dutt1. The two isoforms show differential expression patterns; Dutt1 isoform is widely expressed in development and also is present in adult tissues whereas Robo1 isoform is only expressed

in embryonic brain, eye and kidney tissues (Clark et al. 2002). A recent study demonstrated the differential use of alternative exons and 5'UTR sequences in human and mouse Robo2 (Yue et al., 2006). However, zebrafish alternative exon usage in the predicted exonic regions that correspond to intracellular portion of the Robo2 protein has not been yet performed (see Dalkic et al., 2006 for publication of part of this thesis).

1.2.6. Axon Guidance Molecules and Cancer

Axon guidance molecules that are known to shape neuronal migratory pathways have become emerging candidates for determining the invasiveness and adhesion properties of cancer cells. Axon guidance molecules such as slits, semaphorins and netrins were shown to be expressed outside the nervous system. The genomic localizations of these genes were on frequent loss-of-heterozygosity regions (Chedotal et al. 2005). These proteins and their receptors were suggested to control the vascularization of tumors and regulate cell migration and apoptosis (Chedotal et al. 2005). Axon guidance molecules were demonstrated to have important roles for angiogenesis, a crucial process for tumor growth and metastasis. For instance, semaphorin 4D and its receptor plexin B1 were highly expressed in various tumor cell lines such as breast, colon, prostate, and lung, particularly co-expressed in invasive parts (Basile et al. 2006).

Robo and its signaling components also have been associated with progression of certain cancers. Slit2 was expressed in a human malignant melanoma cell line (Wang et al. 2003). Robo1 was expressed in endothelial cells (Wang et al. 2003); and a recent study implicated Robo1 as a novel hepatocellular carcinoma diagnostic target (Ito et al. 2006). As mentioned earlier, Robo4 was shown to be expressed in the sites of tumor vessels, and it was suggested to have a role in angiogenesis (Huminiecki et al. 2002). Robo1 mRNA level was shown to be upregulated in colorectal cancer whereas Robo4 was shown to be upregulated in the endothelial cells of tumor vessels (Grone et al. 2006). Slit-robo signaling was shown to have a role in mediating the connection between cancer cells and endothelial cells (Wang et al. 2003). In a study, which analyzed expression levels of a variety of axon guidance genes, slits and robos were shown to be

overexpressed in prostate tumors, in contrast to others such as DCC, NEO1, etc.; these findings support the significance of slit-robo signaling among axonal pathway members for cancer progression (Latil et al. 2003). Among a group of 538 candidate genes predictive of inflamatory breast cancer progression, no other axon guidance gene but robo2 was reported to be overexpressed (Bieche et al. 2004). In contrast to these studies, various slit-robo members were shown to undergo promoter hypermethylation and therefore downregulation during cervical cancer, however, this list did not include robo2 (Narayan et al. 2006).

1.3. PI3K/AKT/TOR PATHWAY COMPONENTS AND SIGNALING

1.3.1. Phosphoinositide-3-kinases (PI3Ks)

PI3Ks are lipid kinases that phosphorylate phosphoinositides such that upon activation phosphatidylinositol (4,5)-bisphosphate is converted to phosphatidylinositol(3,4,5)-trisphosphate. PI3K is a heterodimer of p85 kda regulatory subunit and p110 kda catalytic subunit (Carpenter et al. 1990). In CHO-PDGFR and CHO-IR cells, overexpression of all PI3K regulatory subunits results in the downstream phosphorylation of akt1 (Inukai et al. 2001). On the other hand, in CHO-EGFR cells, p85 and p50 regulatory subunites (p85alpha, p85beta, and p50alpha) only lead to PI3K-induced Akt1 (v-akt murine thymoma viral oncogene homolog 1) activation.

1.3.2. v-akt murine thymoma viral oncogene homologs (AKT)

There are three AKT/PKB members in mammals, namely, Akt1, Akt2, and Akt3 (Woodgett et al. 2005). With respect to cancer studies, Akt1 and Akt2 were shown to act in opposite directions when regulating the proliferation of breast epithelial cells. Reductions in Akt2 levels were shown to inhibit the proliferative phenotype observed in MCF-10A cells overexpressing IGF-IR whereas Akt1 inhibition led to their epithelial-mesenchymal transition (Irie et al. 2005). Downstream of Akt/Pkb phosphorylation lies

several substrates, which in turn signal changes in transcription and translation in the cell. These substrates include Bad, Gsk3β, and Foxo proteins (Harrington et al. 2005).

1.3.3. Glycogen synthase kinase 3 beta (GSK3B)

GSK-3 is a serine/threonine kinase, which stays inactivated normally but activated under cellular inhibitory conditions. Upon insulin binding and PI3K activation, PKB/AKT phosphorylation inhibits the Gsk3, resulting in dephosphorylation and activation of glyogen synthase and eIF2B. Alpha and beta isoforms of Gsk have overlapping roles (Patel et al. 2004). GSK-3B was found to be activated upon serum deprivation and preceded apoptosis in neurons (Hetman et al. 2000).

1.3.4. Target of Rapamycin (TOR) Complexes

TOR is the target of rapamycin (Heitman et al. 1991) protein, and is inhibited by rapamycin, a macrolide isolated from *Streptomyces hygroscopicus* with well-known antifungal, immunosuppresive and anti-proliferative properties (Sehgal et al. 1975; Douros et al. 1981; Calne et al. 1989; Sehgal et al. 1998; Huang et al. 2002). Rapamycin acts on TOR protein by inhibiting its role in the regulation of cell growth and division therefore inducing cell cycle arrest or apoptosis. TOR participates in two different complexes that have distinct roles. In the well-known TOR Complex 1 (TORC1), it regulates protein synthesis, whereas in TOR Complex 2 (TORC2) it regulates actin organization; and only TORC1 seems to be rapamycin sensitive (Martin et al. 2005) (Figure 1.1). These complexes are conserved from yeast to mammals although there are two different TOR genes in yeast but single one in vertebrates.

1.3.5. PI3K/AKT/TOR pathway

Rapamycin sensitive-mTOR (mammalian TOR) activity can be regulated by nutrients, growth factors and energy metabolism. For nutrient control, two other factors Raptor and mLST8 (GBL, G protein beta subunit-like) form a complex with mTOR.

Raptor recruits mTOR substrates, S6K1 (RPS6KB1, ribosomal protein S6 kinase, 70kDa, polypeptide 1) and 4EBP1 (EIF4EBP1, eukaryotic translation initiation factor 4E binding protein 1), and is necessary for their subsequent phosphorylation (Beugnet et al. 2003; Choi et al. 2003; Schalm et al. 2003). mLST8 plays a positive role by stabilizing mTOR-Raptor interaction (Kim et al. 2003). In response to nutrient conditions, alterations of the configuration of the mTOR-Raptor-mLST8 complex determine the availability of the targets such as S6K and 4E-BP to mTOR. For control of mTOR by growth factors, there is a linear cascade activity of PI3K, AKT, TSC (tuberous sclerosis), and Rheb (Ras homolog enriched in brain) proteins. Growth factor directed activation of mTOR was shown to be mediated by PI3K (Chung et al. 1994; Mendez et al. 1996). PI3K positively regulates mTOR activity (Cheatham et al. 1994; Chung et al. 1994; Brunn et al. 1996; von Manteuffel et al. 1996; Gingras et al. 1998). PTEN (phosphatase and tensin homolog (mutated in multiple advanced cancers 1)) negatively affects this pathway since it dephosphorylates PIP2 and PIP3 products of PI3K (Neshat et al. 2001; Podsypanina et al. 2001). AKT, a downstream effector of PI3K, also is an enhancer for mTOR activity (Gingras et al. 1998; Verdu et al. 1999; Scanga et al. 2000; Lizcano et al. 2003; Miron et al. 2003). On the other hand, Tsc1/Tsc2 heterodimer acts as a negative regulator of mTOR (Gao and Pan et al. 2001; Potter et al. 2001; Tapon et al. 2001; Gao et al. 2002; Inoki et al. 2002; Jaeschke et al. 2002; Manning et al. 2002; Tee et al. 2002). AKT phosphorylates Tsc2, thereby activating mTOR through inactivation of Tsc1/Tsc2 inhibitors (Potter et al. 2001; Goncharova et al. 2002; Kwiatkowski et al. 2002; Inoki et al. 2002; Manning et al. 2002). Tsc2 exhibits GTPase activity for Rheb, which is placed downstream of Tsc1/Tsc2 and positively regulates mTOR (Saucedo et al. 2003; Stocker et al. 2003; Castro et al. 2003; Garami et al. 2003; Inoki et al. 2003). It is not yet known how Rheb activates mTOR.

In addition to nutrients and growth factors, energy levels have also effect on mTOR (Dennis et al. 2001). Decrease of ATP/AMP ratio is sensed by AMPK (protein kinase, AMP-activated) which in turn hampers mTOR function through Tsc2 activation (Hardie et al. 1998; Kemp et al. 1999; Kimura et al. 2003; Inoki et al. 2003) (Fig. 1.1). Some studies showed crosstalk between nutrient and growth factor induced regulation of

mTOR, specifically through Tsc1/Tsc2 (Tee et al. 2002; Gao et al. 2002; Matsumoto et al. 2002; Garami et al. 2003; van Slegtenhorst et al. 2004). It is not yet known if Raptor and mLST8 have also role in growth factor induced activation of mTOR (Hay and Sonenberg 2004). A recent study implicated the Vps34, a class III PI3K, as the transducer of nutrient availability to mTOR (Dann and Thomas 2006).

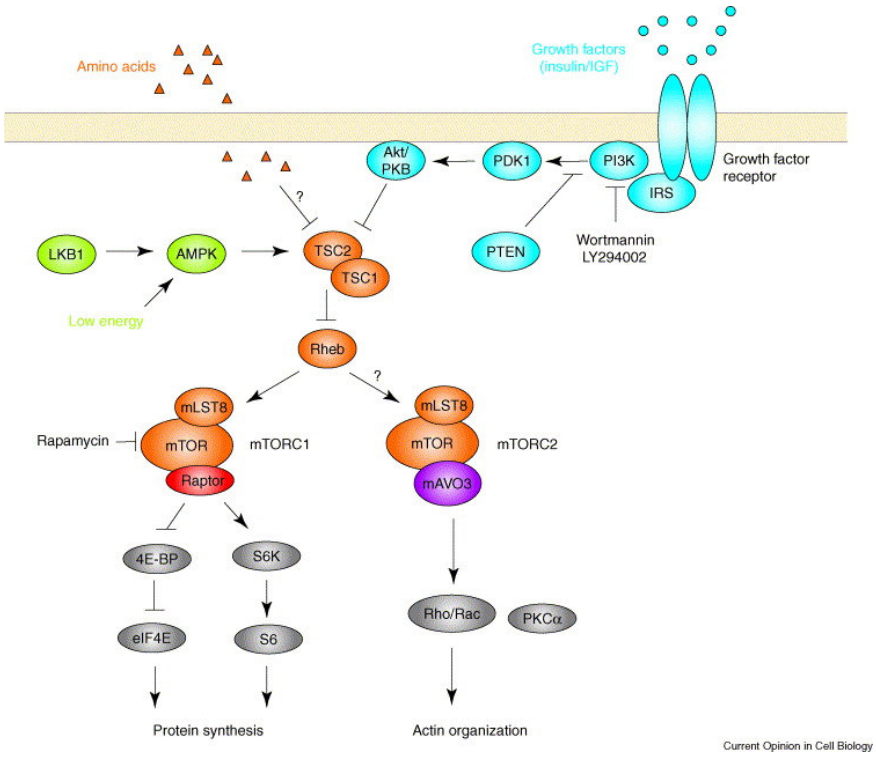

Figure 1.1. TOR signaling network consisting of two complexes (From Martin and Hall 2005).

Major targets of mTOR are 4E-BP (4E Binding Protein) and p70S6K (p70 S6 Kinase). 4E-BP1, the inhibitor of eIF4E (Eukaryotic Initiation Factor 4E), is phosphorylated and inactivated by mTOR (Polakiewicz et al. 1998; Gingras et al. 1998). p70S6K is activated by mTOR (Polakiewicz et al. 1998; Gingras et al. 1998). In addition, mTOR phosphorylates PP2A (Protein phosphatase 2A), therefore prevents 4E-BP and S6K from dephosphorylation (Di Como and Arndt 1996; Peterson et al. 1999).

1.3.6. Serum Starvation and PI3K/AKT/TOR pathway

There is an intricate connection between nutrient deprivation/growth factor signaling and the concomitant modulation of PI3K/AKT/TOR pathway. For example, thyroid hormone (T3) was shown to activate AKT signaling in cardiac myocytes and, and PI3K/AKT/mTOR/S6K altogether in human fibroblasts (Kuzman et al. 2005, Cao et al. 2005). In a study that uses rat nucleus pulposus cells, survival in hypoxic conditions was shown to be correlated with the activation of PI3K/AKT and MEK/ERK (Mitogen-activated protein kinase kinase/Extracellular-regulated MAP kinase kinase) pathways, and inactivation of the Gsk3β. The use of inhibitors of this pathway, LY294002 and PD98059, resulted in impaired survival indicating the significance of these pathways in cellular growth and proliferation (Risbud et al. 2005). Similarly, in cardiac fibroblast cells, serum starvation was shown to induce necrosis and apoptosis. During this event, MAPK (Mitogen-activated protein kinase) and AKT were shown to be downregulated (Leicht et al. 2003).

Several studies showed a connection between serum starvation and cancer. Various cancer cell lines including those of liver, pancreas, gastric, and colon showed higher resistance to serum deprivation when compared with normal human fibroblasts (Izuishi et al. 2000). High level expression of AKT was found to be correlated with this resistance; by using antisense technology and specific inhibitors, a role for Akt1, Akt2 and PI3K was found in the tolerance of cancer cell lines to serum-deprivation (Izuishi et al. 2000). Pten, an inhibitor of PI3K and AKT, was overexpressed in a prostate cancer cell line that normally lacks Pten; this was shown to induce apoptosis that was similarly induced by serum starvation, and resulted in decreased insulin like growth factor receptor cell surface expression (Zhao et al. 2004). Supporting evidence came also from a study with malignant mesotheliomas. Under serum starvation, these cells showed high Akt levels, and homozygous deletion of Pten. Treatment with rapamycin or LY294002 was able to induce growth arrest (Altomare et al. 2005). It was shown that p53 induction resulted in downregulation of mTOR activity as the phosphorylation levels of S6K decreased; an action involving AMPK and TSC complex (Feng et al. 2005). In addition

to this, p53 was transiently phosphorylated in response to glucose starvation (Feng et al. 2005). On the other hand, it was reported that PI3K and TOR inhibitors resulted in a growth arrest phenotype that was different from the serum starvation phenotype (Tresini et al. 1998, Tsurutani et al. 2005).

1.3.7. Bioinformatics for Studying Gene Structure and Expression

With the availability of high-through put techniques genome sequences of a variety of organisms from human to yeast was sequenced or is in the process of sequencing and assembling. Online databases like Ensembl (www.ensembl.org), UCSC Genome Browser (genome.ucsc.edu), etc. are available to search the sequenced genomes. These kind of databases allow us to analyze the genomic structure of genes, including exon-intron splicing juctions, UTRs, etc. These databases include ESTs (Expressed Sequence Tag) that are the sequences known to be expressed at mRNA level. However, these ESTs do not cover all of the expressed sequences and therefore transcripts can contain exons other than the already known ones. Gene prediction programs like Genscan and FgenesH can therefore provide us with some exons that could not have been identified in the previously known transcripts pf genes and thus these tools are used to search for possible alternatively spliced exons.

Microarray is a large scale experimental method to give the mRNA expression profiles of genes genome-wide. They provide a complementray expression profile of genes in a condition specific experiment. There are databases that contain the results of microarray experiments such as stanford database (genome-www5.stanford.edu) and GEO database (www.ncbi.nlm.nih.gov/geo). There are some examples of zebrafish microarrays. Mathavan et al. (2005) have analyzed the embryonic expression pattern of zebrafish from unfertilized stage to 48 hpf embryos using oligonucleotide arrays. Their findings indicated that zebrafish showed coregulated expression of many protein complexes, such as ribosomal protein subunits, proteosome members, and cell cycle regulators. An important advantage of microarray studies is that they provide a gene with its relation to other genes in terms of the expression patterns and if a gene of interest

could be searched for its coexpressed genes. If these coregulated genes fall into specific categories, such as regulation of cell cycle, apoptosis, then one can associate the novel gene with these functions. As an example, in a previous study, promoters and introns of genes were collected genome wide and it was found that 4,852 genes contained sequences for binding to p53 and the significance of this bioinformatic approach was confirmed by expression analysis (Wang et al. 2003). Gene networks are networks that contain connectivity information about genes. The connectivity parameter could be trancriptional regulatory one, a direct interaction one, or simply a coexpression one. A gene coexpression network could be contructed from the result of microarray experiment. A comprehensive study demonstrated the presence of a conserved gene coexpression network among multiple taxa exists (Stuart et al. 2003). In this study, a large amount of microarray data for various organisms from yeast to human was gathered; and genes that are conserved among different organisms and present in the microarray results were designated as Meta-genes and these genes which showed similar expression patterns in a conserved manner were designated as neighbors yielding a conserved coexpression network in the end. As a result, constructing such conserved gene networks allow us to analyze the functional relevance of a gene of interest.

CHAPTER II: AIM AND STRATEGY

2.1. MOTIVATION AND AIM

Robo2 is an attractive candidate for cancer research since it is an important regulator of cellular growth and migration. However, there has been no study up to date that deals with its expression in adult zebrafish tissues as well as its degree of coexpression with members of PI3K/AKT/TOR pathway, an essential mitogenic and cell migration regulator.

Loss of regulation of cell growth and cell division is the key to the progression of cancer. TOR protein, acting downstream of PI3K/AKT/PTEN pathway, has been characterized for its crucial role in the regulation of cell growth and division. Indeed, mitogenic activity of one or more of these aforementioned pathway members has been implicated in tumorigenesis (Tsuratani et al. 2005). Dysregulation of cellular migration is yet another prominent character of tumors, particularly during metastasis. Axon guidance molecules that are known to shape neuronal migratory pathways have become emerging candidates for determining the invasiveness and adhesion properties of cancer cells. Therefore, it is an intriguing possibility that PI3K/AKT/TOR pathway elements may be involved in expressional regulation of axon guidance molecules (e.g., Robo-Slit signaling).

In this study, we particularly focused on Robo2, a gene known to have a repulsive role during axon guidance yet also has been shown to be dysregulated in certain tumors (see Introduction Section 1.2.1 and 1.2.6). The primary aim of this thesis, therefore, was to study adult and larval expression pattern of Robo2 in zebrafish, a well known vertebrate model for human diseases. Moreover, the modulation of expression of Robo2 and selected PI3K/AKT/TOR pathway members in the presence of rapamycin, an mTOR inhibitor, as well as at different levels of serum also were examined.

2.2 . STRATEGY

2.2.1. Computational Approach

2.2.1.1. Prediction of Robo2 Coexpression Neighbors

One possibility to understand which genes are likely to be coexpressed is to use a conserved expression network obtained based on microarray data from multiple taxa. We have chosen meta-gene dataset (Stuart et al. 2003) that is available at http://cmgm.stanford.edu/~kimlab/multiplespecies/index.html. This site allows for searching of a gene of interest with respect to its neighbors, which made identification of coexpression neighbors of Robo2 and mTOR, possible.

Second, we have taken a species-specific signaling pathways approach in which genes of interest such as PI3Ks, AKT, GSK3B, and TOR proteins were involved could be profiled in terms of their embryonic expression; and their coexpression neighbors. Moreover, these pathway-specific genes were clustered with Robo2 expression in the context of PI3K/AKT/TOR pathway.

2.2.1.2. Phylogenetic Analysis

Zebrafish has become a valuable model for comparative genomics studies. To determine expression levels of selected PI3K/AKT/TOR pathway members, it is important to identify the orthologs, accurately. This process requires blast searches of mammalian sequences against the zebrafish genome assemblies. Upon identification of zebrafish orthologs, multiple alignment of the nucleotide and amino acid sequences are required. These alignments also help in selection and design of primer sequences to amplify the products of these selected genes. We aimed to identify zebrafish orthologs of several PI3K/AKT/PTEN/TOR pathway members phylogenetically using public genome databases (e.g., www.ensembl.org) to make candidate gene selection in an accurate manner.

2.2.2. Experimental Approach

2.2.2.1. Tissue and Developmental Expression Profiles

RT-PCR and Real-time RT-PCR are the chosen methods to analyze mRNA levels of interested genes in this study. Since real-time RT-PCR allows for quantitative determination of expression, correlations among expression levels of genes therefore could be assessed precisely.

To study the mRNA expression of Robo2 and other selected target genes in *in vivo* and *in vitro* conditions, we have used zebrafish as a model system due to its short developmental period and ease of maintenance. Accordingly, we aimed to characterize Robo2 expression (and its alternatively spliced forms, if any) in the embryo, larvae, and adult tissues in zebrafish. Furthermore, we aimed to show the presence/absence of any Robo2 isoforms in multiple developmental stages and adult tissues in zebrafish. Conservation of Robo2 isoforms in rat also was important to assess to generalize our conclusions.

2.2.2.2. Transcriptional Response to Rapamycin and Serum Deprivation

To study the degree of correlation between the mRNA expression of Robo2 and those of the selected pathway genes, several treatments (such as rapamycin administration and serum-starvation) known to modulate cell growth/division seemed appropriate choices. Multivariate analyses, such as hierarchical cluster analysis provided a better visualization of these correlations.

CHAPTER III: MATERIALS AND METHODS

3.1. ANIMALS

Zebrafish (*Danio rerio*), purchased from pet-shops or provided by University of Oregon at Eugene, OR, USA (AB strain), or University of Bergen, Norway (Tu/AB) were kept and raised using standard methods. In addition, Sprague-Dawley rats were used from the animal holding facility of Bilkent University.

3.1.1 Maintenance

Fish were maintained under a cycle of 14 hours day and 10 hours night at 28.5^{o}C. Before sacrifice, animals were anesthetized by tricaine solution (0.12% adults, and 0.08% embryos and larvae). Adult fish were dissected by using sterile equipment in order to obtain different tissues. Embryos were collected on the following morning of the setup and maintained in plates filled with system water. Embryos, larvae and juvenile fish were staged according to hours post fertilization (hpf), days post fertilization (dpf) and relevant morphological criteria (Kimmel et al., 1995).

Nine weeks old, 200-250 grams male or female Sprague-Dawley rats were used. They were housed under controlled environmental conditions (22ºC) with a 12-hour light and 12 hour dark cycle in the animal holding facility of Bilkent University, Turkey. All the animals received care according to the criteria outlined in the "Guide for Care and Use of Laboratory Animals" prepared by the National Academy of Science; and this study protocol complied with Bilkent University's guidelines on humane care and use of laboratory animals.

3.1.1.1 Aquaria system and water condition

Zebrafish were kept in glass aquaria filled up with system water. Tap water was allowed to stay for two days before being fed into the system. Each aquarium was equipped with a standard filtering system; 25-40% of the system water was replaced with fresh system water weekly. Illumination period (14 h light/ 10 h dark) was kept constant by using a clock-timer.

3.1.1.2 Housing and feeding

Adult zebrafish were of 3-4 cm length; and up to 15 adults were kept in a 30 liter aquarium with weekly water changes of 25-40 %. Adult fish were fed the dry food flakes twice per day, supplemented with high protein-content granulated food and/or *Artemia nauplia*.

3.1.2 Breeding

To obtain efficient breeding, fish were kept at a constant 14h/10h light/dark regime at 28.5 °C. Pairs of male and female fish were put in the breeding cages in the afternoon; the fertilized eggs were collected in the morning. In our system we were able to obtain 70 to 300 embryos per set-up, and generally up to 50 to 80% of them were viable. Unfertilized eggs were discarded immediately while fertilized eggs were transferred into a 95-mm Petri dish and washed several times in system water.

3.1.3 Embryo handling

Maximum of 70 embryos were kept in 95-mm Petri dishes in embryo medium. Petri dishes were kept in an incubator, set at 28.5 °C with a 14h light/10h dark illumination period. System water was used to work with the embryos. In order to treat multiple embryos either with rapamycin or control solutions, they were transferred into 96-well plates. Within each well, up to 5-10 embryos can be treated by a maximum of

250µl treatment solution. Embryos can be kept in these wells until 5 dpf since they feed from their yolk. Zebrafish older than 6 dpf were kept in 200 ml platic holders with mesh bottoms and were fed baby dry flake (Tetramin).

3.2. CELL CULTURE

ZF4 (ATCC CRL-2050) is a cell line derived from zebrafish embryonic fibroblast cells. ZF4 cells were cultered in D-MEM/F-12 (Invitrogen,11039-021) containing 10% fetal bovine serum with 100 µg/ml Streptomycin/Penicilin at 28ºC in air. Cells were trypsinized and passaged twice a week. Serum starvation experiments were performed for 24 hours; 10%, 3%, 1%, and 0% serum were used for each treatment group, respectively.

3.3. STANDARD SOLUTIONS & BUFFERS

3.3.1. 10X TBE electrophoresis buffer

108 g Tris base
55 g Boric acid
40 mlEDTA(0.5 M)
add dH2O to the 1 liter

3.3.2. 1X TE electrophoresis buffer

10 mM Tris.Cl (pH 7.4)
1mM EDTA

3.3.3. DNA loading buffer

20% glycerol 400
0.25 % bromophenol blue
0.25 % xylene cyanol

3.3.4. Traciane solution (stock)

400 mg tricaine powder

97.9 ml dd H_2O

~2.1 ml 1 M Tris (pH 9).

to use as an anesthetic:

4.2 ml tricaine stock solution

~100 ml clean tank water

3.3.5. PBS

8 g NaCl

0.2 g KCl

1.44 g Na_2HPO4

0.24 g KH_2PO4

dissolve in 800 ml dH_2O, adjust the pH 7.4 with HCl

add dH_2O to 1 liter

3.3.6. DEPC-H_2O

500 µl DEPC (from AppliChem)

1 liter dH_2O

o/n aeration, autoclave

3.4. RAPAMYCIN TREATMENT OF EMBRYOS

Rapamycin (Calbiochem, CA, Cat. No. 553210) purchased as 100 µg or 1 mg solid product was dissolved in DMSO (dimethlysulphoxide) as a stock solution with a concentration of 5 mM; aliquoted into smaller volumes; and was stored at -20°C in dark. Its concentration was then adjusted to 20µM by making an appropriate dilution using the system water. Rapamycin was provided in system water at the appropriate concentration in the wells of 96-well plates. In each experiment, control solutions were prepared by including the same amount of DMSO as found in the rapamycin solutions. At 48 hpf, embryos were removed from wells; either observed and photographed in the depression slide and/or treated with RNAlater solution for further analysis of mRNA expression.

3.5. DETERMINATION OF GENE EXPRESSION

The expression of several genes from embryos, larvae, various adult tissues, and cell line were measured upon isolation of RNA from multiple samples, conversion of RNA into cDNA; and finally by using qualitative PCR and/or real-time quantitative PCR.

3.5.1. Total RNA Isolation

During RNA isolations, all material and solutions were treated with diethyl pyrocarbonate (DEPC) to inhibit the RNase contamination. Larval and adult zebrafish samples were first put into the RNAlater solution or liquid nitrogen; and then total RNA isolation was performed by using the Qiagen RNeasy Mini Kit or alternatively Ambion Totally RNA isolation kit. Briefly, samples removed from RNAlater were put in the RLT buffer, which contains 1% B-ME (β-mercaptoethanol). Samples were homogenized in RLT by using 20 gauge needles; 70% EtOH was added to the homogenized lysate and mixed. 700 µl of the sample were added to an RNeasy mini column in a 2 ml tube; and centrifuged for 15 s at 10.000 rpm. After discarding the flow-through, 700 µl buffer RW1 were added to the RNeasy column, centrifuged for 15 s at 10.000 rpm. Next, 500 µl buffer RPE with 100% EtOH, were added onto the RNeasy column, and centrifuged for 15 s at 10.000 rpm; and this was repeated a second time followed by centrifugation for 1 min at full speed. 30 µl RNase-free water were pipetted on the column in a 1.5 ml collection tube; and centrifuged for 1 min at 10.000 rpm. The elute containing RNA of the sample was stored at -80 C. Alternatively, RNA was isolated by using the Totally RNA Isolation Kit (Ambion) according to manufacturers protocols (Ambion).

For RNA isolation from the ZF4 cell line, cells in culture were first washed with 1X PBS; then trypsinized; and the plate was rocked to detach the cells. After removal of trypsin, and cells were rinsed with 1X PBS. Next, cells were collected, centrifuged at 500 *xg* for 5 minutes and supernatant is discarded to obtain a pellet. RNA was isolated by Promega SV Total RNA Isolation kit accroding to the manufacturers protocols. In brief, 175 µl SV RNA Lysis Buffer was added onto the pellet; homogenized by using 20 gauge

needles. 350 µl SV RNA Dilution Buffer was added to the lysate; mixed by inverting 3-4 times and kept at 70 ^{o}C for 3 minutes. Samples were centrifuged at 13,000 rpm for 10 minutes; and the lysate was then transferred to a microcentrifuge tube; 200 µl 95% EtOH was added and mixed by pipetting 3-4 times. The mixture transferred to a spin column was centrifuged at 13,000 rpm for 1 minute. Next, 600 µl SV RNA Wash Solution was added; and the column was centrifuged at 13,000 rpm for 1 minute before discarding the flow-through. DNase treatment was performed by applying 50 µl Dnase incubation mix onto the membrane; the samples were incubated at RT for 15 minutes. 200 µl SV Dnase Stop Solution was added; centrifuged at 13,000 rpm for 1 minute; and then washed by 600 µl SV RNA Wash Solution by centrifuging at 13,000 rpm for 1 minute. Again, 250 µl SV RNA Wash Solution was added and centrifuged at 13,000 rpm for 2 minutes. Elution was performed by 100 µl Nuclease-Free Water added onto the membrane; the samples were centrifuged at 13,000 rpm for 1 minute; and the resulting RNA solution was kept at -80 ^{o}C.

3.5.2. Determination of RNA Concentrations

2 µl of each sample was diluted (1:200) with 400 µl DEPC-treated ddH_2O. Then, the measurements were taken at 260 nm and 280 nm by using Beckman spectrophotometer. Alternatively 2 µl of RNA solution was used to measure the concentration and O.D ratio by using NanoDrop ND-1000 spectrophotometer. The concentration was calculated by using the formula; [RNA]=O.D260*40*d.f(200).

O.D 260/O.D280 ratio was used for the purification quality of the RNA. For high-quality RNA solutions, it must be between 1.8 and 2.1.

For the visualization of RNA on gel, 4 µl of RNA solution was mixed with 2 µl of DNA Loading Buffer and 10 µl of ddH_2O and incubated at 60 °C for 10 minutes before being loaded into 1% Agarose Gel. The bands were examined under the UV light and images were analyzed by using the Multi-Analyst Software (Bio-Rad, USA).

3.5.3. cDNA Amplification

After the RNA isolation and measurements, equal amounts of the RNA were converted into the 1st strand cDNA by using the Fermentas cDNA kit (Catalog No. 1622). First, RNA was annealed by oligodT primers for 5 min at 70 ^{o}C. Then, the mixture was treated by an RNase inhibitor for 5 min at 37 ^{o}C. Finally, mixture was treated by the MMLV-reverse transcriptase for 1 hour at 42 ^{o}C and 10 min at 70 ^{o}C. The amplified cDNAs were stored at -20 ^{o}C.

3.5.4. Orthology Prediction and Phylogenetic Analysis

Pi3kr2 (PI3K Regulatory subunit 2), Gsk3b, and Akt2 genes were selected as candidate genes coregulated with Robo2 under serum deprivation and growth inhibition by rapamycin conditions. The nucleotide and protein sequences of human PI3KR2, GSK3B, and AKT2 were aligned against to those of zebrafish and other organims for which complete amino acid sequences were reported in NCBI database (www.ncbi.nlm.nih.gov). Multiple alignments were performed using ClustalW 1.8 in BCM Search Launcher (http://www.searchlauncher.bcm.tmc.edu/) and then visualized using BOXSHADE 3.1 (http://www.ch.embnet.org/software/BOX_form.html). Phylogenetic trees were generated by using TreeTop Phylogenetic Tree Prediction online tool (http://www.genebee.msu.ru/services/phtree_reduced.html).

3.5.5 Primer Design

Primers were designed with Primer3 online tool (http://frodo.wi.mit.edu/cgi-bin/primer3/primer3_www.cgi). Each primer pair was blasted against the zebrafish (or rat) genome and mRNA sequences to ensure specificity. Some previous primers had been designed by using a software program, the Primer Designer Version 2.0 (Scientific and Educational Software; Kuscu et al. 2004, MS Thesis). The list of primers used in this study is given in Table 3.1 below together with their sequence.

Table 3.1. Forward and reverse primer sets used to amplify the genes mentioned in the study given in the 5'-3' direction.

Primer Name	**Primer Sequence (5'-3')**
Robo2 NCBI1F	CTCGGCAGCCTGCAGATCAA
Robo2 NCBI2F	AAGACTTCCGCGATGTGATG
Robo2 E21F	CCTTAGTGTCTGACATCGAG
Robo2 E22R	GGACGAGGTCTATGAGGAA
Robo2 AER	ATCATCTTCTGAAGCCGAGC
Robo2 RATF	CCCCTCAGAGCACTAGACCA
Robo2 RATRI	TCCATCCAGCCTAAAACCAG
Robo2 RATRO	TCCCTCCGATGAGGTAACAC
Robo2 MAMF	GAGCACT(G/A)GACCAGAC(T/A)CC
Robo2 MAMRO	T(G/T)GGTCCATCCG(C/T)CCTC
CyclophilinF	GGGAAGGTGAAAGAAGGCAT
CyclophilinR	GAGAGCAGAGATTACAGGGT
MIPEPF	AACATCGAGATCCAGCACC
MIPEPR	ACATCCTCAGAGAATTGCAG
TORF	ACACGCTGCACGCACTGATT
TORR	CCACCTTCTCCATTAGAGTC
PI3KR2F	ACCAGGCAAAGGAAGATCAA
PI3KR2R	GGGTCTGGCTCTCTCTGATG
AKT2F	CTGGCAAGATGTGCTTCAAA
AKT2R	GGGAGAAGTGTGTGCGTGTA
GSK3BF	AACTGCGGGAACCAAATGT
GSK3BR	CTCCACTGTTGGCATCTGAA

3.5.6 RT-PCR

Following the conversion of RNA into cDNA, an RT-PCR reaction was performed with the appropriate primers using the cDNA as a template. PCRs were performed in 0.2ml Thermowell tubes using the Techne PCR machine (Techne, ftGENE2D, Cambridge, UK). Each reaction contained a total of 25 µl reaction volume that includes 1 µl cDNA, 0.5 µl of 20 pmol reverse and forward primers, 0.5 ml 0.2mM dNTP, 1.5 µl 1.5 mM MgCl2, 2.5 µl 10X PCR buffer and 1 unit Taq DNA polymerase (Fermentas, Catalog No. EP0402). PCRs included an initial heating step, then a number of cycles of denaturation, annealing and extension steps was performed. PCRs were finished with a final extension step. For various PCRs different conditions were used as listed in Table 3.2. PCR product was mixed with 5 µl DNA Loading Buffer and 20 µl of this mix was loaded on a 1-2% agarose gel in the electrophoresis system and visualized under UV light.

3.5.7 Real Time RT-PCR

Qiagen Real-Time Kit containing SYBR green as a marker dye for measurement of PCR yield in each cycle was used for all reactions. 12.5 µl SYBR- green mix, 10 pmol forward and reverse primers, and 1 µl cDNA were mixed in the supported 96 well-plate and RNase-free water was added to 25 µl in each well, and 3 µl mineral oil was added at the top of the solution to inhibit the evaporation of the product from the well. PCR reactions were performed using the BIO-RAD iCYCLER machine. For each primer set, PCR program was the same with that explained in the section 3.5.5, but additionally iCYCLER reactions included a pre-activation step for the hot-start Qiagen Taq DNA polymerase (95 ^{o}C for 8-10 min). A melt curve was generated at the end of each set of reactions beginning with 55 ^{o}C and ending at 95 ^{o}C by 0.5 ^{o}C increments in each 15 seconds. Normalized mRNA expression values were calculated by on the ΔΔCt method as proposed by Pfaffl (2001) upon calculation of primer efficiencies based on 10-fold dilution curves.

3.5.8. Analysis of Genomic Structure of Robo2 Homologs

Ensembl genome database was used to analyze the genomic structure of Robo2 gene for zebrafish, human, rat, chicken, dog, and chimpanzee. The relevant sequence accession numbers were provided in the Results section and Figure legends therein. The GenScan predictions were used to detect presence of alternative exons not found in the published EST and transcript information (see Figure 4.1 in Results section). Paralogs of Robo2 in the genomes mentioned above also was searched for the alternative exons under investigation; multiple alignment of sequences were performed using ClustalW (http://www.ebi.ac.uk/clustalw/) and the Logo was generated by WebLogo (http://weblogo.berkeley.edu/)

3.5.9. Analysis of Zebrafish Microarray Data

List of genes that are involved in PI3K, AKT, insulin signaling, GSK3B signaling were obtained from a signaling pathway database Biocarta (www.biocarta.org). Furthermore, Mathavan et al. (2005) dataset was searched for keywords such as *wingless/wnt*, *insulin*, *inositol*, *phosphoinositide*, *phosphatidly*, *frizzled*, *disheveled*, *glycogen*, and *thymoma* in the human homologous gene name column. Pearson correlation coefficients between these genes and Robo2 expression level were calculated and those genes with less than 0.55 (or greater than -0.55) correlation coefficient were excluded. Furthermore, only genes with annotated NCBI Unigene Ids were included in the further analysis (Table 4.5). Along with the expression profile of Robo2, the zebrafish embryonic development expression profiles of these genes (annotated with their potential human homolog gene descriptions) were clustered using Cluster (http://rana.lbl.gov/) and Treeview programs.

Table 3.2. Conditions optimized for the PCR reactions for the candidate genes. Final extension was performed at 72°C for 10 minutes.

PRIMER PAIR	Denaturation	Cycle	Denaturation	Annealing	Extension
NCBI1F-E22R	94°C 5 min.	40	94°C 30 sec.	60°C 30 sec.	72°C 2 min.
NCBI1F-AER	94°C 5 min.	40	94°C 30 sec.	60°C 30 sec.	72°C 2 min.
NCBI2F-E22R	94°C 5 min.	40	94°C 30 sec.	60°C 30 sec.	72°C 2 min.
NCBI2F-AER	94°C 5 min.	40	94°C 30 sec.	60°C 30 sec.	72°C 2 min.
E21F-E22R	95°C 5 min.	30	95°C 30 sec.	58°C 30 sec.	72°C 30 sec.
E21F-AER	95°C 5 min.	30	95°C 30 sec.	58°C 30 sec.	72°C 30 sec.
RATF-RATRI	95°C 5 min.	30	94°C 30 sec.	55°C 30 sec.	72°C 30 sec.
RATRF-RATRO	95°C 5 min.	30	94°C 30 sec.	58°C 30 sec.	72°C 30 sec.
MAMF-MAMRO	95°C 5 min.	35	95°C 30 sec.	55°C 30 sec.	72°C 30 sec.
MIPEPF-MIPEPR	95°C 5 min.	30	95°C 30 sec.	58°C 30 sec.	72°C 30 sec.
CYCF-CYCR	95°C 5 min.	25	95°C 30 sec.	58°C 30 sec.	72°C 30 sec.
TORF-TORR	95°C 5 min.	30	95°C 30 sec.	59-60°C 30 sec.	72°C 30 sec.
AKT2F-AKT2R	95°C 5 min.	30	95°C 30 sec.	59°C 30 sec.	72°C 30 sec.
PI3KR2F-PI3KR2R	95°C 5 min.	30	95°C 30 sec.	59°C 30 sec.	72°C 30 sec.
GSK3BF-GSK3BR	95°C 5 min.	30	95°C 30 sec.	59°C 30 sec.	72°C 30 sec.

CHAPTER IV: RESULTS

4.1. ALTERNATIVE SPLICING OF ROBO2

4.1.1. Comparison of Zebrafish and Rat Robo2 Sequences

Complete zebrafish *robo2* genomic sequence is currently unavailable. Ensembl database contains a predicted transcript (Ensdart00000014877; www.ensembl.org; WTSI Zv5) partially corresponding to zebrafish *robo2* (NM_131633). Several NCBI zebrafish ESTs, which aligned primarily to the 5' and 3' ends of the *robo2* cDNA sequence (NM_131633) also could be detected (CK686381.1, AL920855.1, CN173823.1, CN318984.1, AI437295.1). Exon/intron structure of Ensdart00000014877 in the genomic assembly was analyzed in further detail by comparing with the corresponding Genescan prediction. The most 3' end of Genscan00000032249 exhibited a potential alternative exon, (30^{th} exon; 4508 bp-4693 bp) which was further pursued in the present study (Figure 4.1a).

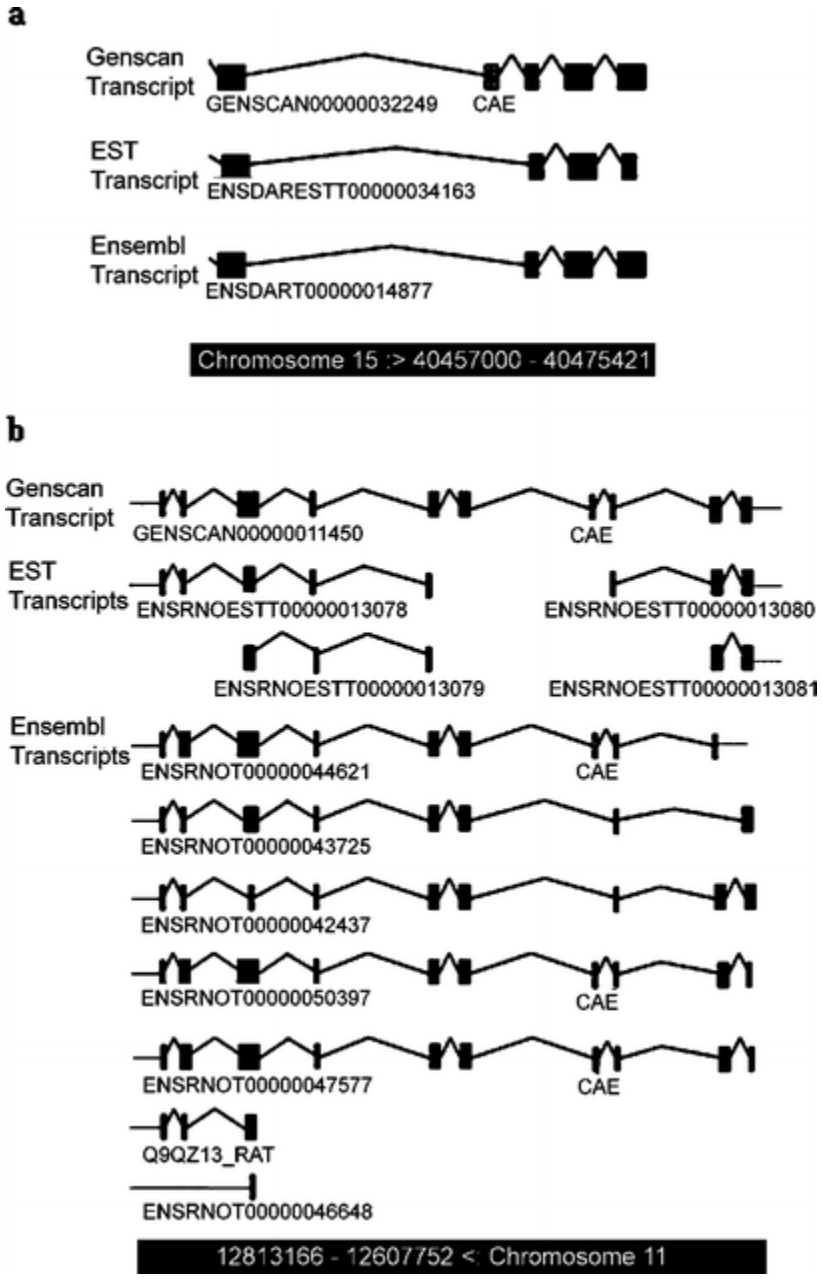

Figure 4.1. The exon/intron structure of Ensembl Transcripts **a** The exon/intron structure of ENSDART00000014877 which corresponds to 3' of zebrafish robo2 is shown in detail (www.ensembl.org). The putative exons (PE) present in the Genscan but not found in the reported transcript are highlighted with open boxes; the conserved alternative exon (CAE) is highlighted in a bold open box **b** The exon/intron structure of Ensembl transcripts corresponding to 3' of rat robo2 is shown in detail (www.ensembl.org). CAE is highlighted in a bold open box.

Full length rat *robo2* mRNA sequence was computationally predicted by NCBI (XM_213677). In the Ensembl database, several computationally predicted isoforms, which differed in their length and their usage of alternative exons including the rat homolog of CAE (Ensrnot00000044621, Ensrnot00000043725, Ensrnot00000042437, Ensrnot00000050397, Ensrnot00000047577, Ensrnot00000046648, Q9QZI3_RAT; Chromosome 11), have been reported (Figure 4.1b).

The human, rat, chimpanzee, dog, and chicken homologs of the zebrafish *robo2* protein sequences were extracted from public databases (GenBank, www.ncbi.nlm.nih.gov; Ensembl, www.ensembl.org). The distant homology search of the zebrafish CAE (Conserved Alternative Exon) of Genscan00000032249 also was performed using the genomic assemblies of these species (www.ensembl.org). Orthologs of CAE mapped, in general, to Genscan predicted putative exonic sites near the 3' end of robo2 (Human: Genscan00000045332, 20^{th} exon: 3081 bp-3263 bp; chimpanzee: Genscan00000073054, 1st exon: 1 bp-183 bp; dog: Genscan00000000765, 24^{th} exon: 3590 bp-3773 bp) for all species examined, except chicken and rat. For chicken, Ensembl provided two transcripts, Ensgalt00000025020 and Ensgalt00000025021, among which Ensgalt00000025021 (8^{th} exon: 1200 bp-1383 bp) contains a sequence highly orthologous to zebrafish CAE. In rat, *robo2* CAE already was annotated as transcribed based on computational prediction algorithms although not shown experimentally (Figure 4.1b).

4.1.2. Multiple Alignment of Robo2 Sequences

Multiple alignment of robo2 orthologous sequences indicated that the protein sequence of zebrafish CAE was highly similar to that of human (80%), chimpanzee (80%), rat (80%), dog (78%), and chicken (80%) CAE (Figure 4.2), whereas the residues from 5′ and 3′ neighboring exons were not as highly conserved (5′ exon: 62% to human, 62% to chimpanzee, 62% to rat, 63% to dog, and 68% to chicken; 3′ exon: 43% to human, 43% to chimpanzee, 33% to rat, 43% to dog, and 41% to chicken). CAE is predicted to yield an in-frame insertion without stop codons (Figure 4.2). It corresponds

to a region between the second and the third cytoplasmic domains (between the 1,311th and 1,312th residues of NM_131633) of the zebrafish robo2 protein sequence.

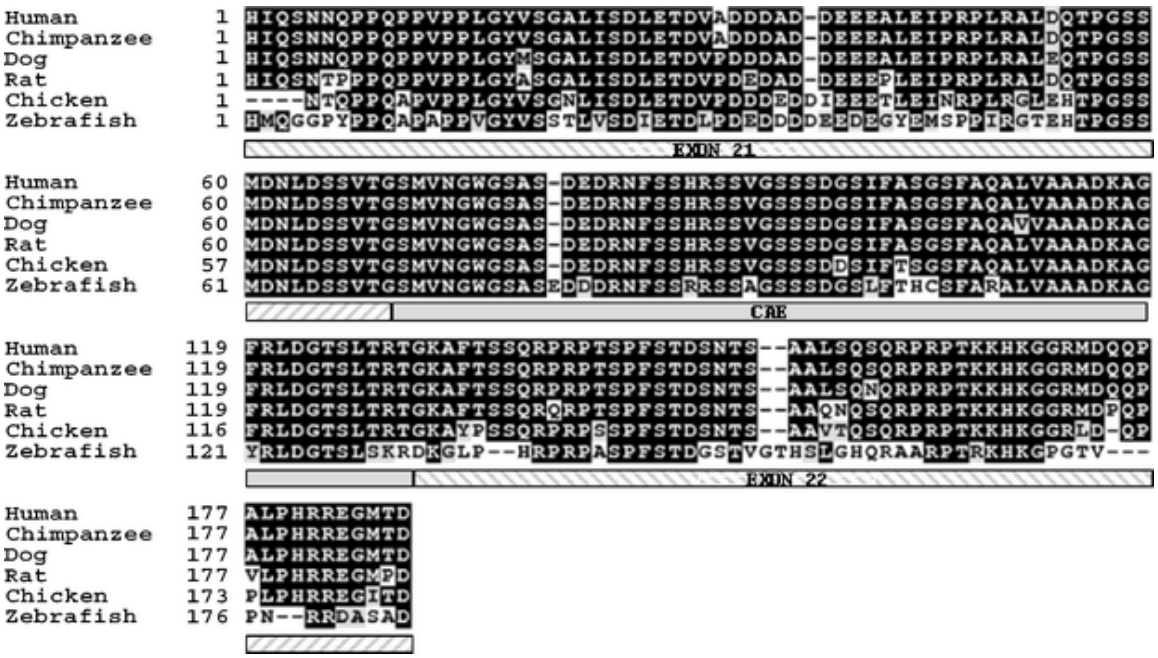

Figure 4.2. Multiple alignment of the robo2 protein sequences for the human, rat, chimpanzee, dog, chicken, and zebrafish was performed using ClustalW 1.8 in BCM Search Launcher (http://www.searchlauncher.bcm.tmc.edu/) and then visualized using BOXSHADE 3.1 (http://www.ch.embnet.org/software/BOX_form.html). The conserved alternative exon has been manually translated and incorporated into the protein sequence when not included in the original NCBI database sequences. The accession numbers and location of the amino acid used at the first position of the alignment are given for each species in parentheses: human robo2 (NP_002933; 1,186), rat robo2 (XP_213677; 1,313), chimpanzee robo2 (XP_516591; 1,121), dog robo2 (XP_544815; 1,186), chicken robo2 (ENSGALP00000024974; 1,073), and zebrafish robo2 (NP_571708; 1,242). The location of CAE and those of the exons 21 and 22 are depicted using *shaded boxes*

CAE also was conserved between paralogs robo1 and robo4, among different vertebrate taxa (Figure 4.3a). Robo1, robo2, and robo4 proteins all possessed a highly

conserved motif (Figure 4.3b) exhibiting greater sequence similarity within the members of a particular paralog (e.g., a paralog-specific submotif: S*MV*NGWGSAS for robo2, S*MI*NGWGSAS for robo1, and S*LA*BGWGSAS for robo4). On the other hand, the conserved motif shown in Figure 4.3 was not present in robo3 in any of the organisms.

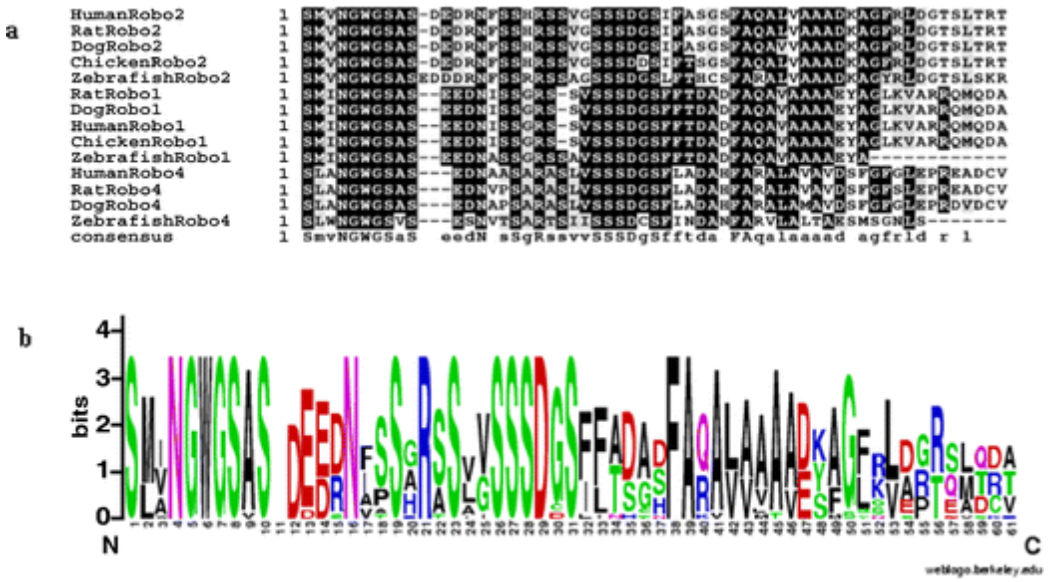

Figure 4.3. Multiple alignment of robo proteins and weblogo representation **a** Multiple alignment of the protein sequences of robo proteins from different species. Human: robo1 (NP_002932, residues 1369–1426), robo4 (NP_061928, residues 872–929); rat: robo1 (NP_071524; 1,369–1,426), robo2 (XP_213677; 1,382–1,441), robo4 (NP_852040; 890–947); dog: robo1 (XP_544814.2; 1,420–1,477), robo4 (XP_546424.2, 912–969); zebrafish: robo1 (NP_571556; 1,388–1,434), robo4 (AAQ10890; 1,014–1,064); and chicken: robo1 (XP_416673; 1,690–1,747). The first position shown in the alignment corresponds to the initial residue given in the parentheses above. Robo2 CAE sequences are as previously described in Figure 1. The last row of the multiple alignment refers to a consensus sequence. No protein sequence with high similarity to the consensus motif could be identified for chicken robo4 in the genome; thus, the chicken robo4 sequence is not aligned. **b** CAE motif highly conserved among robo paralogs

4.1.3. Expression of Robo2 Isoforms in Adult Zebrafish Tissues

The expression of the transcripts of potential *robo2* isoforms encompassing CAE was investigated in a series of zebrafish adult tissues including the eye, heart, spleen, digestive tract, gills, and dorsal fin together with that of a housekeeping gene *mipep* (mitochondrial intermediate peptidase) (Figure 4.4). Our findings demonstrated that CAE was either skipped or included depending on the tissue type; this produced two alternative forms herein called *robo2_tv1* and *robo2_tv2*, respectively (Figure 4.4b). In many of the non-neuronal tissues, *robo2_tv2* was expressed at detectable levels while *robo2_tv1* was predominantly expressed in the eye. Furthermore, the expression of these isoforms was either very low or absent in zebrafish heart (Figure 4.4b).

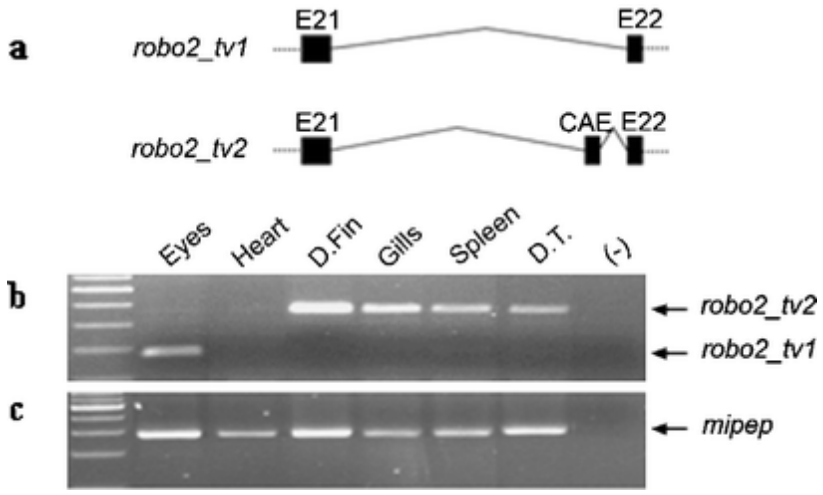

Figure 4.4. Genomic representation and differential expression of robo2 alternative isoforms in zebrafish adult tissues. **a** Genomic representation of *robo2* isoforms with or without the CAE. **b** RT-PCR results with primers E21F–E22R (Table 3.1) on various tissues of zebrafish adults are shown. The expected size of the amplicon is 172 bp when the alternative exon, CAE, is spliced out while amplicon size increases to 358 bp when CAE is included. The *top band* of the 100 bp DNA Ladder Plus corresponds to 600 bp. **c** The RT-PCR of the same tissues also was performed for amplification of mipep as a house-keeping gene (expected size, 318 bp) using MIPEP F-R primers

As *robo2_tv1* and *robo2_tv2* seem to be differentially expressed in neuronal and non-neuronal tissues of zebrafish, brain and liver were used as representative tissues for subsequent experiments. The differential expression pattern of *robo2_tv1* and *robo2_tv2* in liver and brain was confirmed in RT-PCR reactions performed with three different 5′ forward primers, two of which targeted the extracellular portion of robo2 protein and one targeted the exon 21 preceding the CAE (Figure 4.5). Our findings indicated that CAE was highly expressed in liver while its expression was absent or negligible in brain (Figure 4.5e–g), whereas *robo2_tv1* was predominant in brain (Figure 4.5a–c). Sequencing of both the *robo2_tv1*- and the *robo2_tv2*-specific PCR products obtained from zebrafish brain and liver tissue cDNAs confirmed the alternative pre-mRNA splicing of CAE in zebrafish (DQ481484, DQ481485). The presence of alternative splicing events concerning exons other than CAE has not been tested in this study; thus, it cannot be excluded. In general, *robo2_tv2* expression was predominantly present in multiple non-neuronal tissues whereas zebrafish *robo2_tv1* isoform could be characterized as neurally enriched although not necessarily neurally restricted.

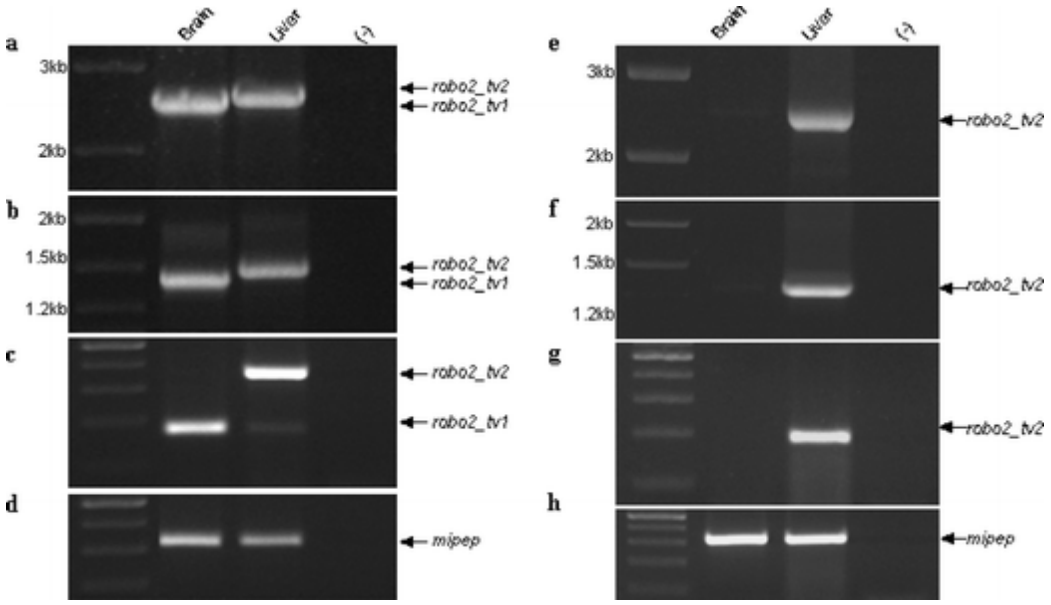

Figure 4.5. The expression of *robo2_tv1* and *robo2_tv2* isoforms on zebrafish brain and liver tissues. **a** Amplification with forward primer NCBI1F (NM_131633; 1,593–1,613) and the reverse primer E22R. Expected sizes of *robo2_tv1* and *robo2_tv2* are 2,534 and 2,720 bp in brain and liver, respectively. The *first lane* corresponds to DNA Ladder Plus. **b** Amplification with NCBI2F (NM_131633; 2,692–2,712) and the reverse primer E22R. Expected sizes of *robo2_tv1* and *robo2_tv2* are 1,435 and 1,621 bp in brain and liver, respectively. The *first lane* corresponds to DNA Ladder Plus. **c** Amplification with the forward primer E21F (NM_131633; 3,955–3,974) and the reverse primer E22R (NM_131633; 4,108–4,126). Expected sizes of *robo2_tv1* and *robo2_tv2* are 172 and 358 bp in brain and liver, respectively. The *first lane* corresponds to DNA Ladder Plus; maximum size shown is 500 bp. **d**, **h** RT-PCR of the same tissues performed using MIPEP F-R primers (Table 3.1). The *first lane* corresponds to 100 bp DNA Ladder; maximum size shown is 500 bp. **e** Amplification with forward primer NCBI1F (NM_131633; 1,593–1,613) and the reverse primer AER (Table 3.1). Expected sizes of *robo2_tv2* is 2,547 bp in liver. The *first lane* corresponds to DNA Ladder Plus. **f** Amplification with forward primer NCBI2F (NM_131633; 2,692–2,712) and the reverse primer AER. Expected size of *robo2_tv2* is 1,448 bp in liver. The *first lane* corresponds to DNA Ladder Plus. **g** Amplification with the forward primer E21F (NM_131633; 3,955–3,974) and the reverse primer AER. Expected size of *robo2_tv2* is 185 in liver. The *first lane* corresponds to DNA Ladder Plus; maximum size shown is 500 bp

4.1.4. Expression of Robo2 Isoforms in Embryo, Larvae and Juvenile Zebrafish

Considering that the relative amount of *robo2_tv1* and *robo2_tv2* expression varied among adult tissues, the possibility of differential expression during embryogenesis and at larval–juvenile stages was also assessed (Figure 4.6). Our results indicated that *robo2_tv2* expression exhibited a dramatic increase starting from the mid-larval stages while it was hardly detectable during embryogenesis or early larval stages (Figure 4.6a, 4.6b). *Robo2_tv1* expression, present at higher levels during embryonic and early larval stages, also displayed an induction later in development (Figure 4.6a).

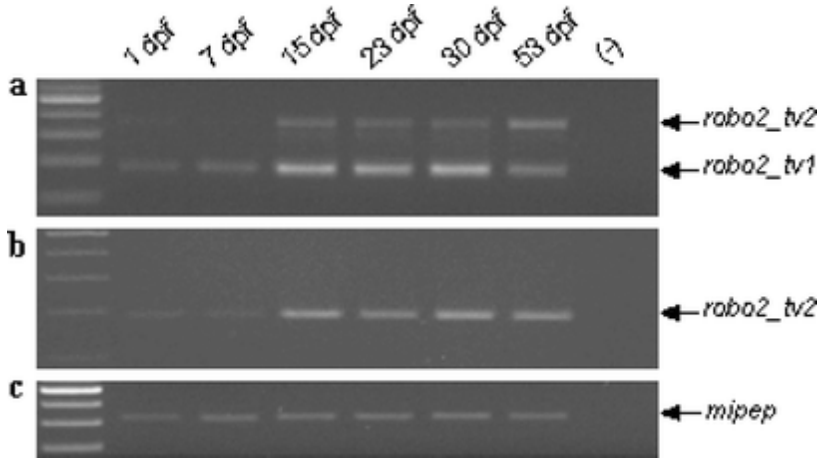

Figure 4.6. The expression of *robo2* isoforms during zebrafish development. **a** RT-PCR results with the primer pair E21F–E22R (expected amplicon sizes 172 and 358, with and without CAE, respectively) performed on cDNAs from various stages: 1, 7, 15, 23, 30, and 53 dpf. The *first lane* corresponds to 100-bp DNA Ladder Plus (maximum size shown, 600 bp). **b** Amplification of RT-PCR results performed on the same set of cDNAs using the primer pair E21F–AER, AER reverse primer specifically targeting a region within CAE. A 100-bp DNA Ladder Plus (maximum size shown, 500 bp) was used. **c** RT-PCR of the same tissues was also performed with MIPEP F-R primers. The *first lane* corresponds to 100-bp DNA Ladder Plus (maximum size shown, 500 bp)

4.1.5. Expression of Robo2 Isoforms in Zebrafish Cell Culture

We further analyzed the expression of robo2 isoforms in zebrafish cell culture ZF4 as our later experiments would include cell culture studies in addition to *in vivo* studies. We observed that robo2_tv2 was expressed in higher levels than robo2_tv1 isoform (Figure 4.7). We confirmed the presence of the alternative splicing event of *robo2* in the cell culture, therefore validated the usage of ZF4 for further studies.

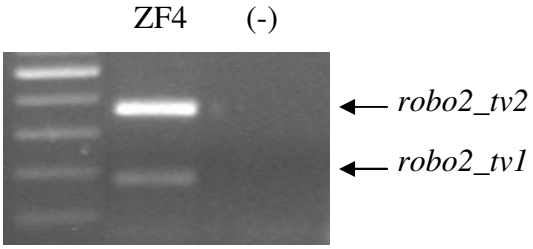

Figure 4.7. The expression of *robo2* isoforms in ZF4**.** RT-PCR result with the primer pair E21F–E22R (expected amplicon sizes 172 and 358, with and without CAE, respectively) performed on a cDNA for ZF4 grown under normal conditions. The *first lane* corresponds to 100-bp DNA Ladder Plus (maximum size shown, 500 bp)

4.1.6. Expression of Robo2 Isoforms in Adult Rat Tissues

Rat *robo2* mRNA (XM_213677) was reported to include the homolog of the zebrafish CAE, although some of the Ensembl-predicted isoforms differed in their usage of it (Ensrnot00000044621, Ensrnot00000043725, Ensrnot00000042437, Ensrnot00000050397). To determine whether *robo2* is also differentially and alternatively expressed in rats, RT-PCR from several rat tissues, including brain, skeletal muscle, heart, liver, spleen, kidney, lung, testes, and ovary was performed with rat-specific primers, RATF and RATRO (Figure 4.8; Table 3.1). Our results demonstrated that, although the rat homolog of CAE (Figure 4.8a) was transcribed in most of the tissues examined, exon skipping was observed to a greater degree in brain and testes

(Figure 4.8b). On the other hand, the CAE exclusion and inclusion events were comparable to each other in the ovary (Figure 4.8b). In addition, nested PCRs on these PCR products performed with the alternative exon-specific primer pair, RATF and RATRI (Table 3.1), yielded the expected product (Figure 4.8c). These findings support the predictions reported in Ensembl in regards to differential incorporation of the rat CAE in *robo2* transcripts (DQ481486, DQ481487).

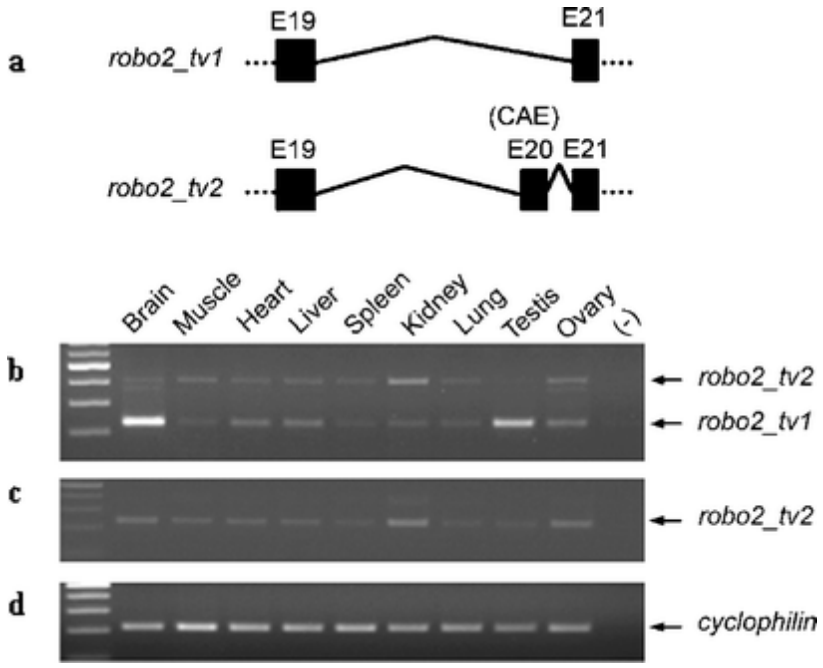

Figure 4.8. Genomic representation and differential expression of robo2 alternative isoforms in rat. **a** Genomic representation of *robo2* isoforms **b** RT-PCR result with primers RATF–RATRO, where RATF targets E19 and RATRO targets E21, on various rat tissues is shown. Expected sizes of the rat *robo2_tv1* and *robo2_tv2* are 224 bp and 407 bp, respectively. The *first lane* corresponds to 100 bp DNA Ladder Plus (maximum size shown, 600 bp). **c** Nested PCR result performed with primers RATF–RATRI, where RATRI targets CAE (i.e., E20) in **a**, using the reactions from RATF–RATRO PCR of **b** (expected band size, 228 bp). A 100-bp DNA Ladder Plus (maximum size shown, 500 bp) was used. **d** RT-PCR of the same samples performed with *cyclophilin* F-R primers. A 100-bp DNA Ladder Plus (maximum size shown, 500 bp) was used

4.2. CONSERVATION AND mRNA EXPRESSION ANALYSES OF PI3K/AKT/TOR PATHWAY MEMBERS IN ZEBRAFISH

Conservation and expression analysis of TOR gene in zebrafish was done previously (Kuscu, C. 2004. MS Thesis). Most of the exons of human TOR was shown to be significantly conserved in zebrafish. The expression levels in embryo and adult stages were also shown (Kuscu, C. 2004. MS Thesis). Therefore, we focused on Pik3r2 (R2 subunit of Pik3), Akt2 and Gsk3b genes of zebrafish in this study.

4.2.1. Phylogenetic Analyses of PI3K/AKT/TOR Pathway Members

Conservation of Pik3r2, Akt2 and Gsk3b in zebrafish was examined by alignment of amino acid sequences obtained from NCBI database with human sequences. As shown in Table 4.8, all the investigated proteins were significantly conserved in zebrafish.

Table. 4.1. Alignment score of the amino acid sequences of PI3K/AKT/TOR members between human and zebrafish.

	Danio rerio **Accession #**	***Homo sapiens*** **Accession #**	**ClustalW Score**
PI3KR2	NP_997987	NP_005018	60
AKT2	NP_937789	NP_001617	86
GSK3B	NP_571456	NP_002084	94

Phylogenetic analysis of Akt2, Pik3r2, and Gsk3b showed that the sequence similarities between zebrafish *(Danio rerio*) and other taxa varied depending on the protein. While Akt2 and Gsk3b were highly conserved especially among vertebrates, zebrafish Pik3r2 protein sequence significantly diverged from those of mammalian and lower taxa (Figures 4.9.1a-c) Rodent sequences were most closely related to each other in each protein; human orthologs of each of the three proteins were evolutionarily closer to their counterparts in rodents than to that in zebrafish, as expected (Figure 4.9.2).

Zebrafish Akt2 and Gsk3b were most closely related to those of *Xenopus leavis* (Figure 4.9.2) while protein sequence of Gsk3b of chordate *Ciona intestinalis* was as distant as that of *Drosophila melanogaster* to all vertebrate taxa, indicating rapid diversion of Gsk3b in fish, amphibians, and mammals (Figure 4.9.2).

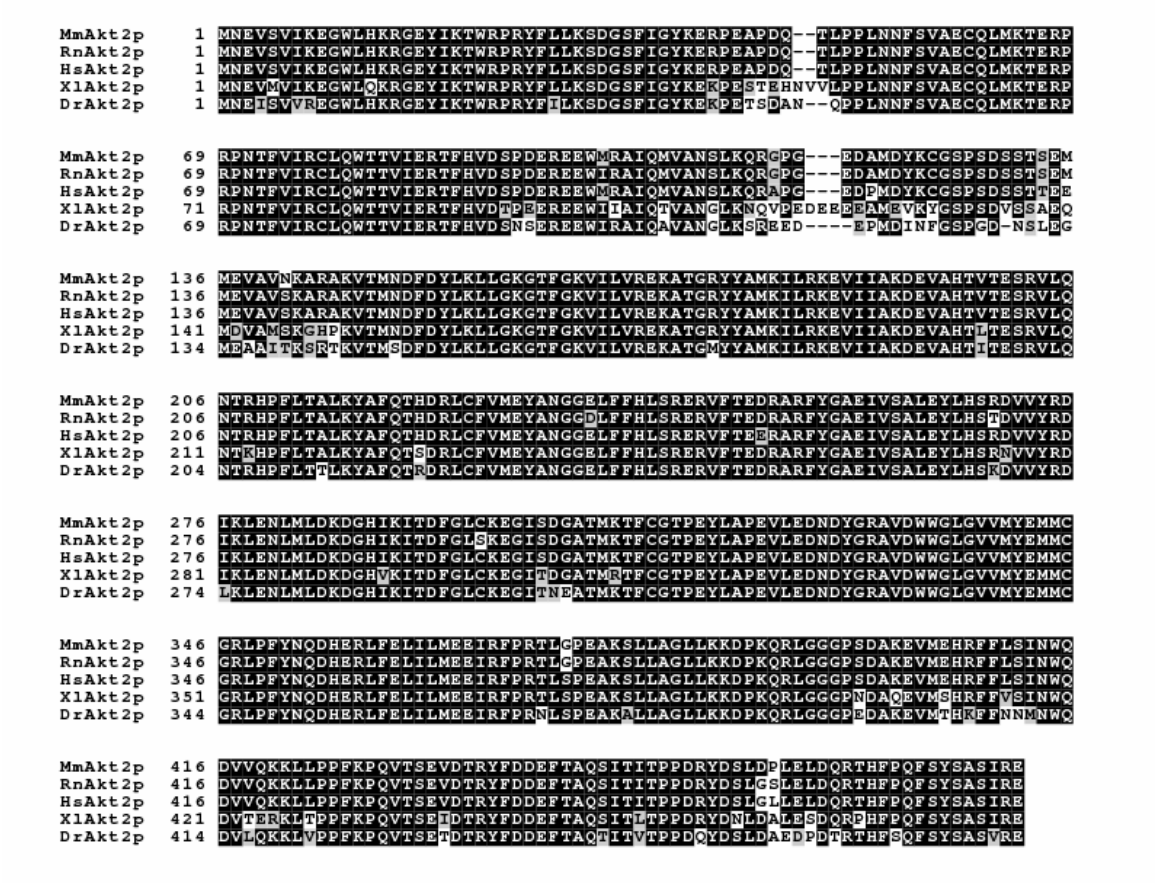

Fig. 4.9.1a. Multiple alignment of amino acid sequences of Akt2 from different taxa. Human and zebrafish sequence accession numbers are given in Table 4.1. Other accession numbers are mouse AKT2 (NP_031460), rat AKT2 (NP_058789), and frog (AAH46261.1).

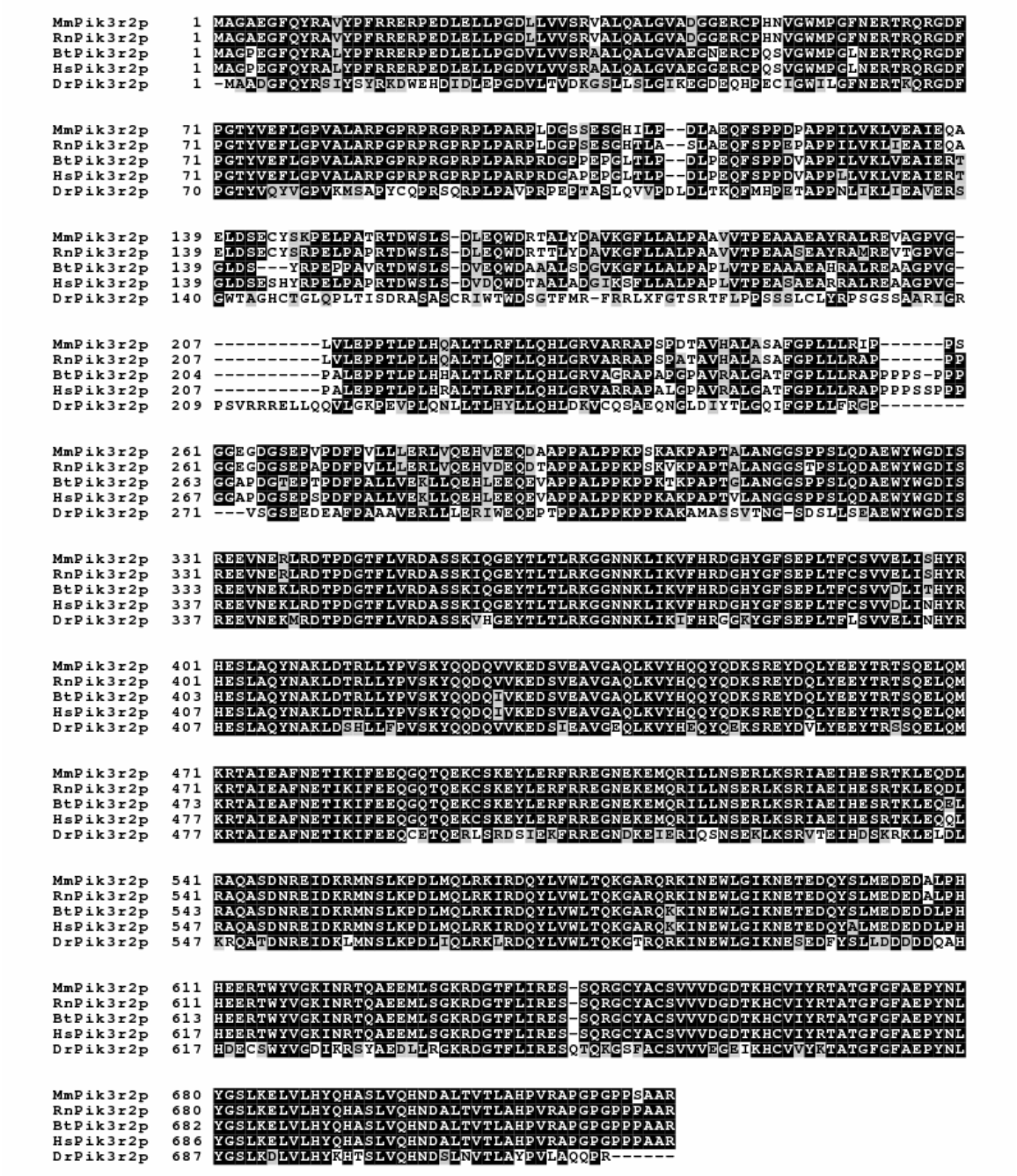

Fig. 4.9b. Multiple alignment of amino acid sequences of Pik3r2 from different taxa. Human and zebrafish sequence accession numbers are given in Table 4.1. Other accession numbers are rat PIK3R2 (NP_071521), mouse PIK3R2 (NP_032867), cow PIK3R2 (NP_777001), rat GSK3B (NP_114469).

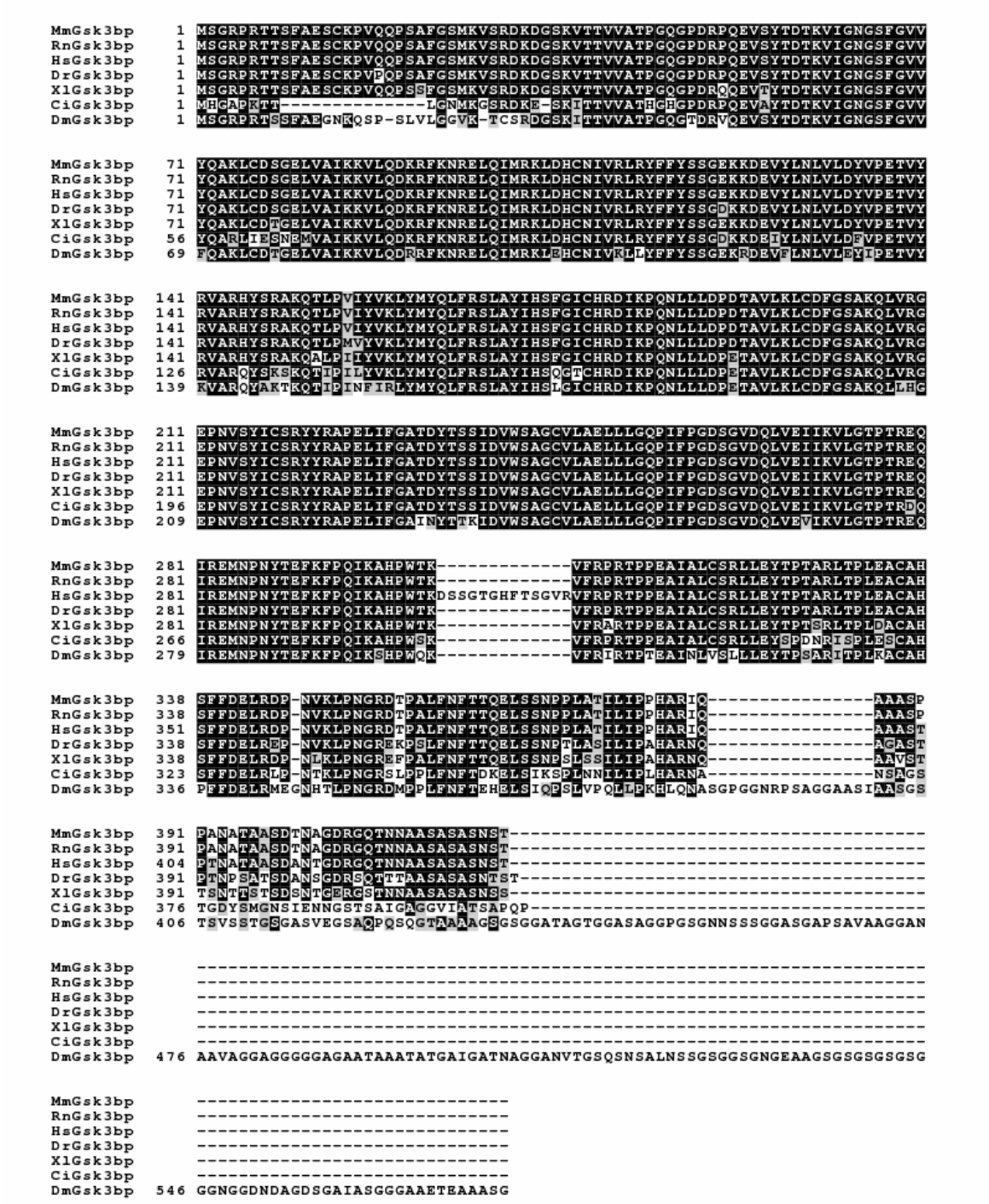

4.9.1c Multiple alignment of amino acid sequences of Gsk3b from different taxa.Human and zebrafish sequence accession numbers are given in Table 4.1. Other accession numbers are rat Gsk3b (NP_114469), mouse Gsk3b (NP_062801), *Ciona intestinalis* Gsk3b (NP_001027597), *Drosophila melanogaster* Gsk3b/shaggy isoform A (NP_476714)

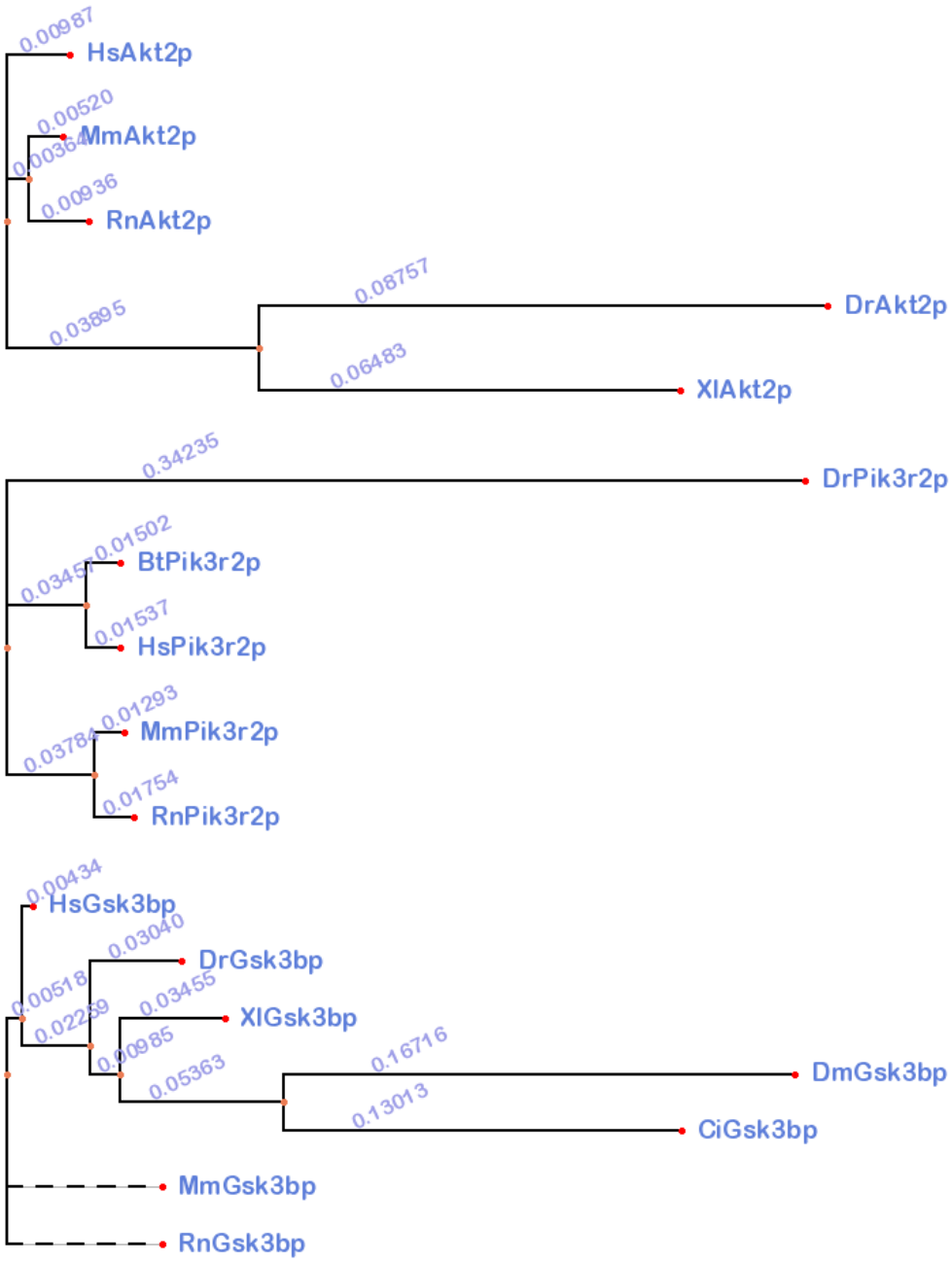

Fig. 4.9.2. Phylogenetic trees obtained from multiple alignment of amino acid sequences shown in Fig. 4.9.1a-c. Trees were generated by phyfi (http://cgi-www.daimi.au.dk/cgi-chili/phyfi/go).

4.2.2. Expression of PI3K/AKT/TOR Pathway Members in Adult Zebrafish

The mRNA expressions of Pik3r2, Akt2, Gsk3b were analzed by RT-PCR on a selected set of adult zebrafish tissues (Figure 4.10).

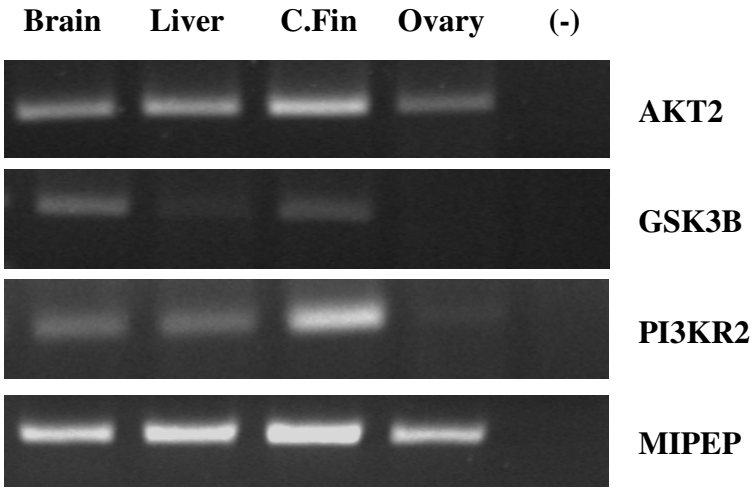

Figure 4.10. Expression of Akt2, Gsk3b and Pik3r2 in adult zebrafish. RT-PCR result with Akt2, Gsk3B, Pik3r2 and Mipep primer pairs from cDNAs converted from mRNAs isolated from adult zebrafish brain, liver, caudal fin and ovary were shown.

All three genes were expressed in almost all of the tissues examined. Akt2 was ubiquitously expressed in brain, liver and caudal fin rather equally but lowly in ovary. Gsk3b was expressed relatively highly in brain and at much lower levels, if any, in other tissues. Pik3r2 was similarly expressed in all tissues except ovary (Figure 4.10).

In summary, selected PI3K/AKT/TOR pathway members were shown to be conserved with respect to their sequences; and they were expressed in zebrafish. All of these genes were pursued in quantitative RT-PCR experiments for the analysis of their expression changes together with Robo2 more accurately in rapamycin and serum starvation experiments.

4.3. LINKS BETWEEN ROBO2 AND PI3K/AKT/TOR PATHWAY MEMBERS

4.3.1 Analysis of Meta-Gene Coexpression Networks

A comprehensive study, which brought together a high number of microarray data from various divergent organisms (Stuart et al. 2003, see Strategy Section 2.2.1.1.) was selected to identify the potential link between Robo2 and the PI3K/AKT/TOR pathway members. Stuart et al. (2003) study provides a highly connected gene coexpression network data, which can be used to analyze the conserved neighbors of selected genes, i.e., Robo2 and Hipk3 (Table 4.2), the only neighbor of Tor, respectively (Tables 4.3 and 4.4). Robo2 had a higher number of neighbors, which included HIPK3 (Table 4.3). Therefore, coexpression neighbors of HIPK3 OR HIPK2 also was provided and discussed as potential coexpression targets of Robo2 (Table 4.4).

Table 4.2. Conserved Neighbors of TOR according to data of Stuart et al. 2003 were listed together with their short descriptions.

Gene Name in Human	Short Description
HIPK3	**homeodomain interacting protein kinase**

Table 4.3. Conserved Neighbors of Robo2 according to data of Stuart et al. (2003) were listed together with their short descriptions.

Gene Name in Human	Short Description
SPTA1	spectrin, alpha, erythrocytic 1
ATBF1	AT-binding transcription factor 1
SEC14L1	(S. cerevisiae)-like 1
C1orf34	-
PLA2G3	misshapenNIK-related kinase isoform 3
GNAI1	G protein, alpha inhibiting activity polypeptide 1
SSH3BP1	spectrin SH3 domain binding protein 1
MAP3K5	MAPERK kinase kinase 5
HIPK3	**homeodomain interacting protein kinase 3**
HOXB7	homeo box B7
TCF8	transcription factor 8
GNB5	guanine nucleotide-binding protein
LAMB1	laminin, beta 1 precursor
AUTS2	gene trap ankyrin repeat
NLGN4	-
CHSY1	lectomedin-2

Table. 4.4. Conserved Neighbors of HIPK3 according to data of Stuart et al. (2003) were listed together with their short descriptions.

Gene Name in Human	Short Description
GNAI1	guanine nucleotide binding protein
C1orf34	-
KIAA0481	cerebral protein
PKC	protein kinase C
FRAP1(TOR)	**FK506 binding protein 12-rapamycin associated protein 1**
KIAA0780	gene amplified in squamous cell carcinoma 1
ACK	activated p21cdc42Hs kinase
MGC21111	misshapenNIK-related kinase isoform 3
ROBO2	**involved in axon guidance**
GRF2	guanine nucleotide-releasing factor 2
GATA3	Member of a GATA family of Zinc-finger transcription factors
PPP1R12C	May mediate protein-protein interactions
KIAA1247	-
EPS15	epidermal growth factor receptor pathway substrate 15
Apbb1ip	May mediate protein-protein interactions
ABR	active breakpoint cluster region-related protein isoform b
TIGD2	decapping enzyme hDcp2
PRKWNK1	protein kinase, lysine deficient 1
MAP3K5	MAPERK kinase kinase 5

Therefore, these data derived from a conserved coexpression network generated by Stuart et al. (2003), linked Robo2 and TOR through the neighborship of HIPK3, hence supported that Robo2 and TOR could be coexpressed and therefore could have functional relation in cellular pathways.

4.3.2. Analysis of Pathway-Specific Gene Expressions

Pairwise correlation coefficients were calculated in order to determine the genes that were correlated with Robo2 expression during zebrafish developmental course microarray data (Mathavan et al. 2005; Table 4.5). Our findings indicated that Robo2 gene clustered together with several Wnt/Frizzled members as well as the members of the TOR pathway (Rheb, Pp2A). The members of this cluster exhibited relatively high correlation coefficients suggesting that Robo2 might be regulated by genes that also regulate TOR pathway (Figure 4.11). Accordingly, several members of the Wnt/Beta_catenin pathway members along with Rheb and PP2A components were upregulated soon after fertilization along with Robo2. Their expression remained rather high until 48 hpf, at which hatching occurs (Figure 4.11). There are other genes in this cluster yet the increase in their expression after fertilization was not as drastic yet they were all up regulated at 48 hpf embyros. These genes included the Gsk3 component Gsk3-alpha, several heat shock members, and the cytoskeletal regulators, actin related protein complex 2/3 members and Rhoae (Figure 4.11). Apart from these positive correlations, Robo2 seemed to be negatively correlated with genes that act along with and downstream of PI3K/AKT (e.g., Bad, Rsk2) and also some members of the Wnt signaling (Axin1 and Dvl3) (Figure 4.12). In this case, all these genes exhibited a rather drastic decrease after fertilization which lasted through the 48 hpf. (figure 4.12).

Table 4.5a. List of genes that are involved in PI3K/AKT/TOR pathway from Mathavan et al. (2005) that are positively correlated with Robo2 mRNA expression.

Accession #	Gene	Unigene Dr	Unigene Hs	Gene Name	Correlation
AB032264	gsk3a	Dr.259	Hs.466828	Glycogen synthase kinase 3 alpha	0.61
AF039412	fzd8a	Dr.8830	Hs.302634	Frizzled homolog 8 (Drosophila)	0.65
AF068772	hsp90ab1	Dr.31066	Hsp83	The structural gene for the 83,000 dalton heat-shock protein (HSP83)	0.66
AF068773	hsp90a	Dr.610	Hsp83	The structural gene for the 83,000 dalton heat-shock protein (HSP83)	0.58
AF114262	foxo5	Dr.8209	Hs.220950	Forkhead box O3A	0.56
AF169639	fzd9	Dr.10341	Hs.31664	Frizzled homolog 10 (Drosophila)	0.64
AF304130	robo1	Dr.11719	Hs.13640	Roundabout, axon guidance receptor, homolog 1 (Drosophila)	0.62
AF336123	fzd7a	Dr.4823	Hs.173859	Frizzled homolog 7 (Drosophila)	0.66
AF337035	robo2	Dr.12403	Hs.13305	Roundabout, axon guidance receptor, homolog 2 (Drosophila)	1.00
AI588708	rheb	Dr.36394	Hs.490576	Ras homolog enriched in brain	0.67
AI878244	ppp2r1a	Dr.5633	Hs.467192	Protein phosphatase 2 (formerly 2A), regulatory subunit A (PR 65), alpha isoform	0.69
AI942574	arpc5a	Dr.15424	Hs.518609	Actin related protein 2/3 complex, subunit 5, 16kDa	0.80
AI959074	rhoae	Dr.18762	Hs.247077	Ras homolog gene family, member A	0.69
AW127776	pak1	Dr.7629	Hs.435714	P21/Cdc42/Rac1-activated kinase 1 (STE20 homolog, yeast)	0.80
AW171089	ppp2r1a	Dr.5633	Hs.467192	Protein phosphatase 2 (formerly 2A), regulatory subunit A (PR 65), alpha isoform	0.63
AW173877	arpc1a	Dr.3270	Hs.124126	Actin related protein 2/3 complex, subunit 1A, 41kDa	0.66
AW203061	arpc5a	Dr.15424	Hs.518609	Actin related protein 2/3 complex, subunit 5, 16kDa	0.66
BF157490	ppp2r1a	Dr.5633	Hs.467192	Protein phosphatase 2 (formerly 2A), regulatory subunit A (PR 65), alpha isoform	0.69
BI672150	ywhabl	Dr.4607	Hs.279920	Tyrosine 3-monooxygenase/tryptophan 5-monooxygenase activation protein, beta polypeptid	0.74
BI880201	ppp2r2b	Dr.12813	Hs.193825	Protein phosphatase 2 (formerly 2A), regulatory subunit B (PR 52), beta isoform	0.62
BI887133	ctnnb2	Dr.28281	Hs.476018	Catenin (cadherin-associated protein), beta 1, 88kDa	0.55
U41081	ctnnb1	Dr.10259	Hs.476018	Catenin (cadherin-associated protein), beta 1, 88kDa	0.71
Z22762	foxa2	Dr.483	Hs.155651	Forkhead box A2	0.73

Table 4.5b. List of genes that are involved in PI3K/AKT/TOR pathway from Mathavan et al. (2005) that are negatively correlated with Robo2 mRNA expression.

Accession #	Gene	Unigene Dr	Unigene Hs	Gene Name	Correlation
AB032262	axin1	Dr.8294	Hs.512765	Axin 1	-0.75
AB041734	dvl3	Dr.10697	Hs.388116	Dishevelled, dsh homolog 3 (Drosophila)	-0.55
AI816679	foxm1l	Dr.17623	Hs.239	Forkhead box M1	-0.58
AI964259	rps6ka3	Dr.12365	Hs.147119	Ribosomal protein S6 kinase, 90kDa, polypeptide 2	-0.69
AJ005691	jak2b	Dr.8116	Hs.434374	Janus kinase 2 (a protein tyrosine kinase)	-0.58
AW059384	nfkb2	Dr.13012	Hs.73090	Nuclear factor of kappa light polypeptide gene enhancer in B-cells 2 (p49/p100)	-0.60
AW116649	prkcsh	Dr.1099	Hs.512640	Protein kinase C substrate 80K-H	-0.65
AW594947	rhoad	Dr.15949	Hs.247077	Ras homolog gene family, member A	-0.58
BG303641	rps6kal	Dr.811	Hs.368153	Ribosomal protein S6 kinase, 90kDa, polypeptide 6	-0.70
BI705519	rhogc	Dr.1709	Hs.501728	Ras homolog gene family, member G (rho G)	-0.59
BI867065	bad	Dr.28	Hs.370254	BCL2-antagonist of cell death	-0.71
BI886921	axin1	Dr.17733	Hs.512765	Axin 1	-0.65
BM026002	pitpna	Dr.12713	Hs.7370	Phosphatidylinositol transfer protein, beta	-0.61
BM082805	pi4kII beta	Dr.14727	Hs.443733	Phosphatidylinositol 4-kinase type-II beta	-0.77
BM102747	nfkb2	Dr.13012	Hs.73090	Nuclear factor of kappa light polypeptide gene enhancer in B-cells 2 (p49/p100)	-0.55

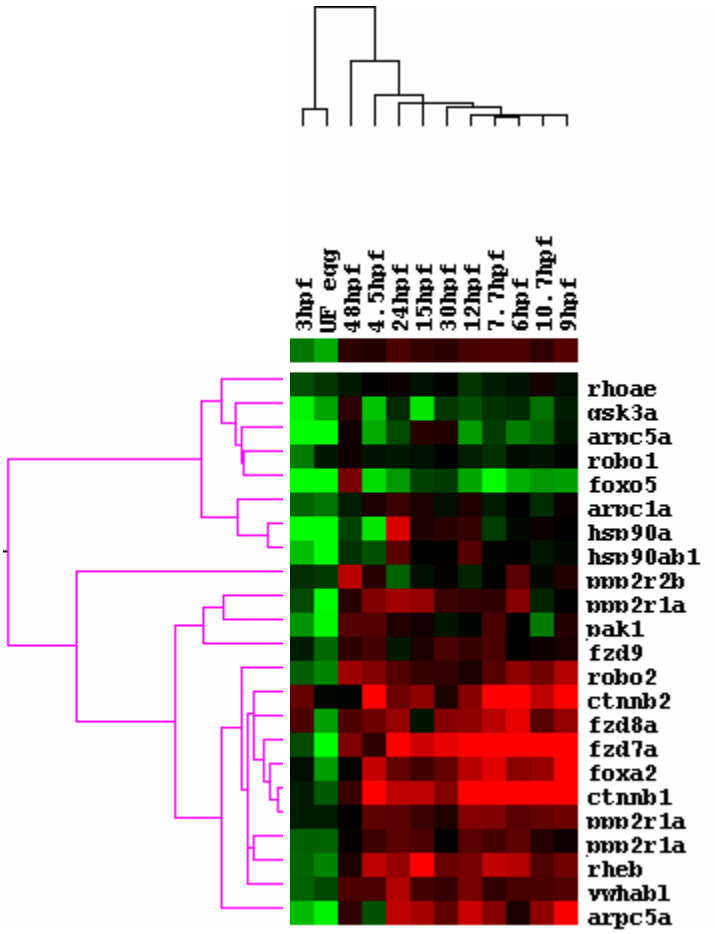

Figure 4.11. PI3K/AKT/TOR pathway related genes that fall into the same cluster with Robo2 (Mathavan et al., 2005 dataset).

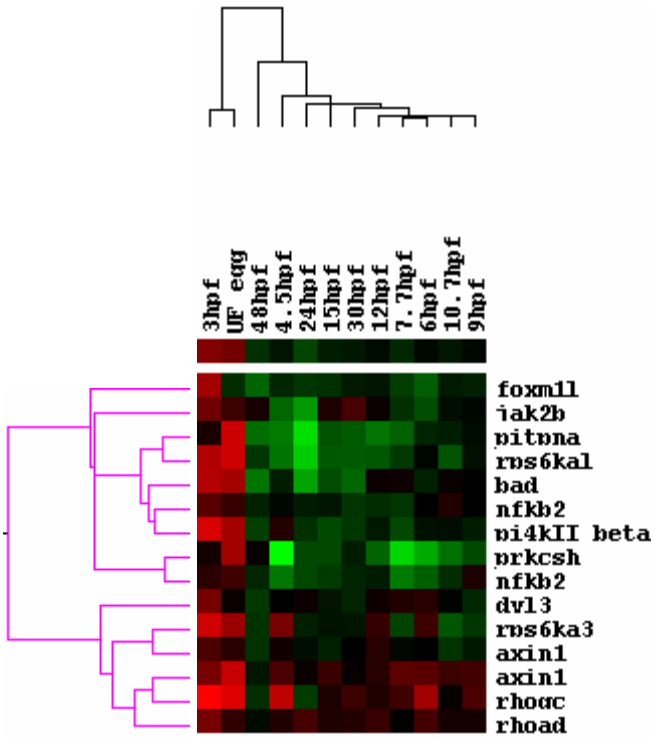

Figure 4.12. PI3K/AKT/TOR pathway genes in Mathavan et al. 2005 dataset that are downregulated during differentiation from 4.5 hpf and longer.

4.3.3. Determination of Primer Efficiencies for Real-Time PCR

For Tor, Robo2, Mipep, Pi3kr2, Akt2 and Gsk3b genes, which were chosen to be analyzed for their alterations in rapamycin and serum starvation experiments, 10-fold dilution curves were obtained (iCycler, Biorad). The slopes obtained from the standard curves of dilution series threshold values were used to calculate the amplification (doubling) efficiencies (Table 4.6). The amplification efficiencies ranged between 1.88 and 2.09, which were within an acceptable range of the expected theoretical value of 2.

Gene Name	**Amplification Efficiency**
Mipep	1.88
Tor	2.06
Robo2	1.94
Pi3kr2	2.09
Akt2	2.09
Gsk3b	1.92

Table 4.6. Amplification Efficiencies of interested genes are given.

4.3.4. Rapamycin experiments

The expression changes of a number of genes in cDNAs belonging to zebrafish embryos treated with rapamycin were analyzed. It was shown previously that rapamycin treatment of zebrafish embryos yielded a phenotype that was characterized by a general growth retardation with unconsumed yolk. Furthermore, pigmentation of the embryos also was reduced (Kuscu, C. 2004. MS Thesis). In 2-days old zebrafish embryos treated and untreated with rapamycin, the expression levels of various genes belonging to PI3K/AKT/TOR pathway and Robo2 were examined by using real-time RT-PCR. The experiments were repeated three times; in each experiment, the treatment or control

groups included 3-5 embryos as sample pools, each. The experiments were performed with pet-shop purchased long-fin, AB strain, and AB/Tub strain embryos, respectively, thus represent information from multiple strains, hence have high variability. Melting curve analysis has shown that for Mipep, Tor, Pik3r2, Akt2, and Gsk3b, each PCR product was unique and of the expected size (Figure 4.13). Among the two robo2 isoforms, in zebrafish embryos robo2_tv1 was more abundant with respect to robo2_tv2, therefore real-time RT-PCR amplified predominantly the robo2_tv1 when using the primer pair E21F-E22R (Figure 4.14). When the primer pair E21F-E21R was used, the real time PCR reaction sometimes produced a dimer together with the expected product although in certain cases the product was free of dimerization (Figure 4.14). Therefore, the expression of Robo2_tv2 could not be accurately quantified in this study. Mean expression fold changes observed upon treatment with 20µM rapamycin have shown a specific profile in which Gsk3b, Robo2, and Pik3r2 exhibited a higher magnitude of change (Figure 4.15). However, due to the large amount of variability in the observed gene expression, none of these fold differences were found to be significant at the level of $p = 0.05$ or lower yet the trend was rather specific (Table 4.7) such that Gsk3b, Robo2, and Tor tended to increase while Pik3r2 was more likely to decrease.

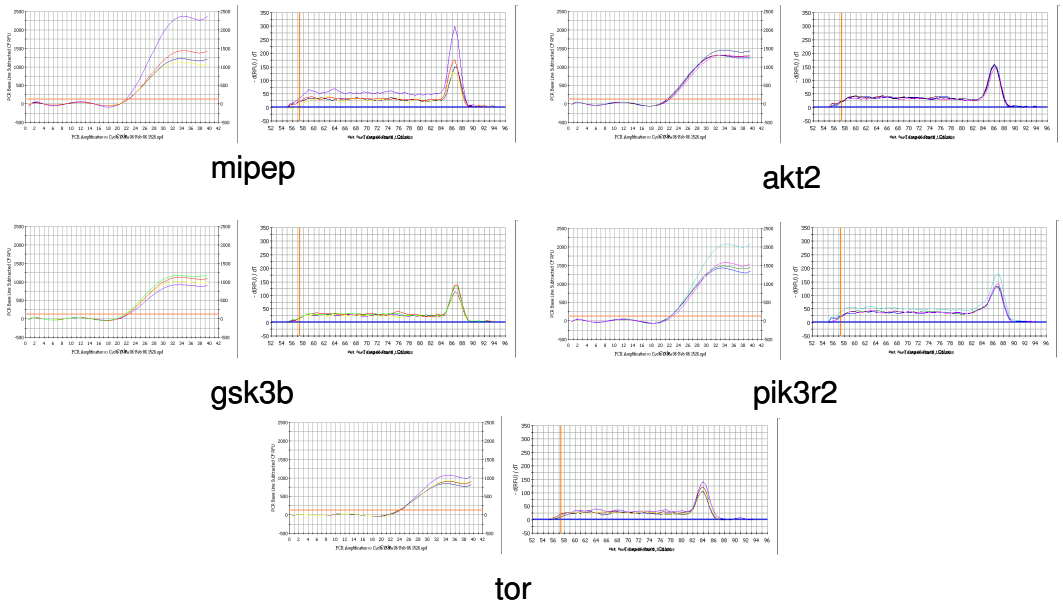

Figure 4.13. Example amplification and melting curves for the selected PI3K/AKT/TOR pathway genes from the rapamycin experiments.

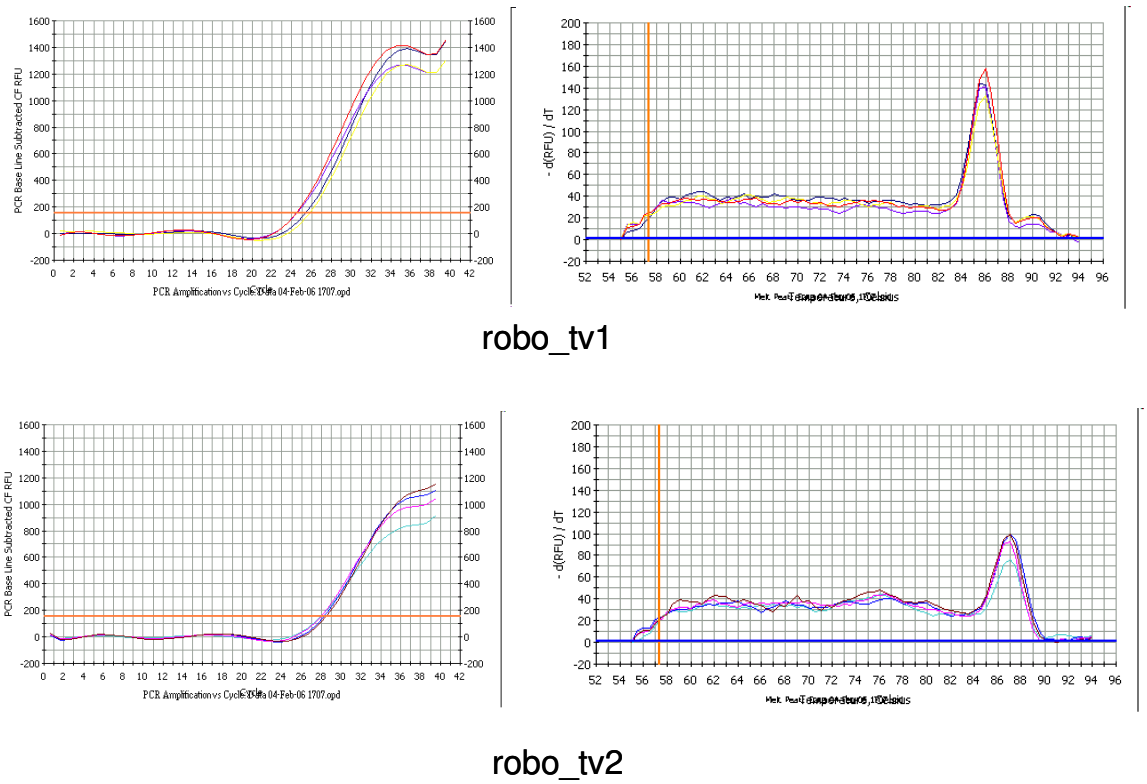

Figure 4.14. Example amplification and melting curves for Robo2_tv1 and Robo2_tv2 mRNA from the rapamycin experiments.

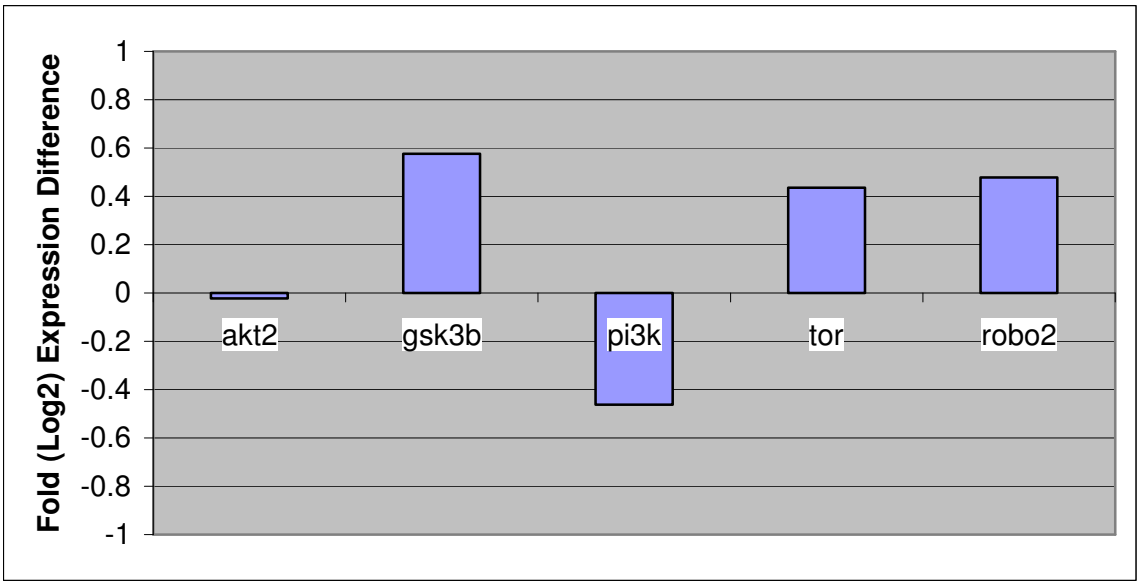

Figure 4.15. Mean expression changes of akt2, gsk3b, pi3k, tor and robo2 genes in response to rapamycin.

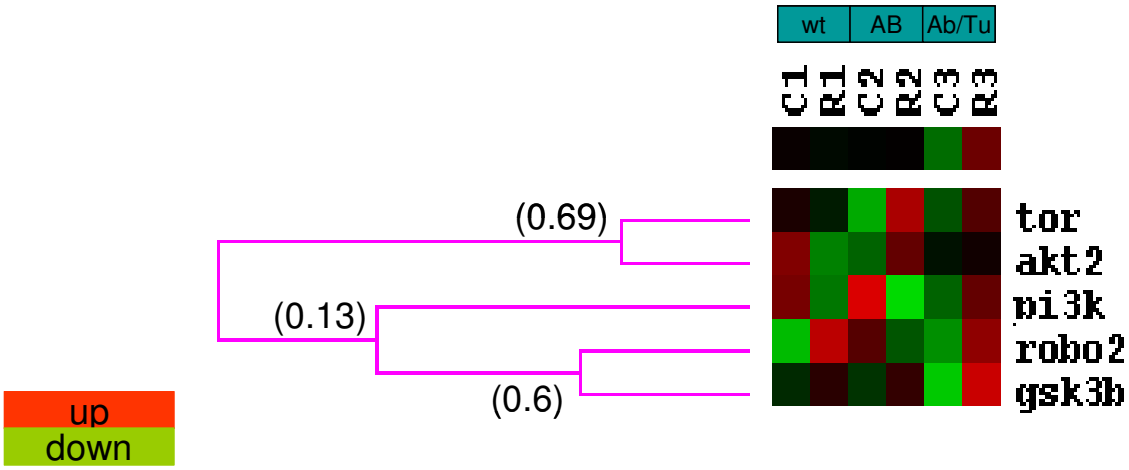

Figure 4.16. Hiearchical clustering of Akt2, Pik3r2, Robo2_v1, Gsk3b, and Tor based on the normalized expression response to rapamycin in 48 hpf old embryos. In paranteses, clustering coefficients were indicated.

Data were clustered hierarchically (Figure 4.16); some of the observed clustering coefficients were around 0.6-0.7, yet they were not statistically significant due to low sample size. None of the genes exhibited statistically significant differences in response to rapamycin.

Table 4.7. Expression changes of akt2, gsk3b, pi3k, tor and robo2 genes in response to rapamycin. Values from each experiment, mean, standard deviations and t-test p-values are listed.

	akt2	gsk3b	pi3k	tor	robo2
Experiment 1	-0.7518	0.244389	-0.69862	-0.16896	1.094933
Experiment 2	0.576994	0.303593	-1.27561	1.003703	-0.50548
Experiment 3	0.108706	1.179468	0.587282	0.472985	0.84395
Mean	-0.02203	0.575817	-0.46232	0.435911	0.477802
STD	0.673973	0.523615	0.953664	0.587208	0.860742
Paired ttest	0.96	0.1971	0.4895	0.3273	0.4378

4.3.5. Expression Profiling under Serum Starvation

We analyzed the expression levels of ZF4 cells that were exposed to serum starvation for 24 hours (Figure 4.17). All genes except Robo2 exhibited a single unique amplicon therefore could be quantified. Robo2_tv1 and Robo2_tv2 were both present in zebrafish cell line ZF4 quite abundantly, therefore it was not possible to use the E21F-E22R primer pair which has led to the amplification of two bands (Figure 4.17). Similarly, a large amount of dimer amplification in Robo2_tv2 specific primer pair E21F-EAE could not be used as in the case of rapamycin experiments.

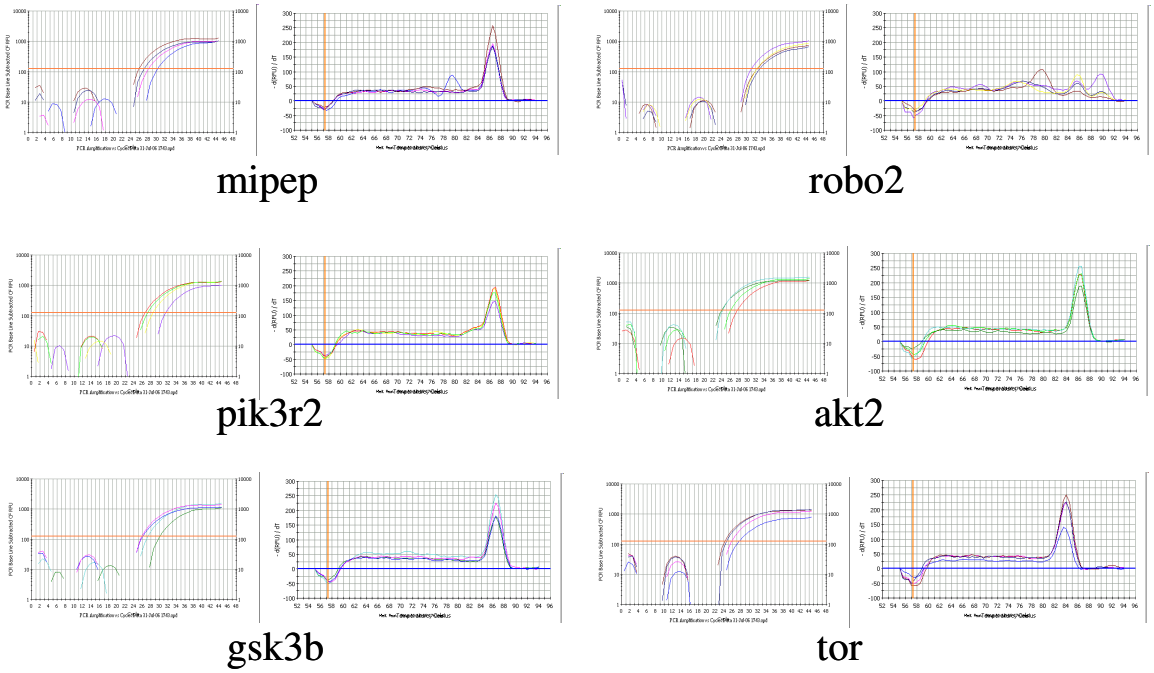

Figure 4.17. Example amplification and melting curves for the selected PI3K/AKT/TOR pathway genes from the serum starvation experiments. Note the ampliciation of both robo2 isoforms with the E21F-E22R primer pair.

Quantitative RT-PCR provided us with the expression alterations in Akt2, Pik3r2, Gsk3b, and Tor genes in response to serum deprivation. ZF4 cells were exposed to 3%, 1% and 0% serum together with a control of 10% (Table 4.8; Figure 4.18). RNA of this experiment was converted to cDNA twice, and each one was analyzed separately to

increase the reliability of the expression readings (Table 4.8). Expression changes of akt2, gsk3b, pi3k and tor genes were examined under these conditions with regard to the reference gene, mipep (Table 4.8). Our findings indicated that there is variability in the expressions that may be partly due to measurements made on different cDNA batches although they were from the same RNA. On the other hand, Pik3r2 was consistently down at 0% in both sets whereas the other genes did not drastically change their expression. Robo2 expression could not be quantified due to the fact that E21F-E22R primers amplified both isoforms which could compete with each other therefore although measurements were taken, they were not considered reliable (Table 4.8; Figure 4.17).

Table 4.8. The normalized fold changes for the serum deprivation experiment.

Experiment	Serum %	Akt2	Gsk3b	Pik3r2	Tor	Robo
set1_1	**10**	0.402	-0.168	0.153	-0.4708	-1.134
	3	0.645	0.026	1.460	-0.236	-0.934
	1	-0.937	-0.505	-0.122	0.126	0.888
	0	0.292	0.479	-1.338	0.110	*0.046*
set1_2	**10**	0.963	0.939	0.928	0.40555	-1.0078
	3	0.083	-0.342	0.366	-0.270	-0.953
	1	-0.147	0.532	0.456	0.065	-0.766
	0	0.064	-0.190	-0.822	0.205	*1.720*

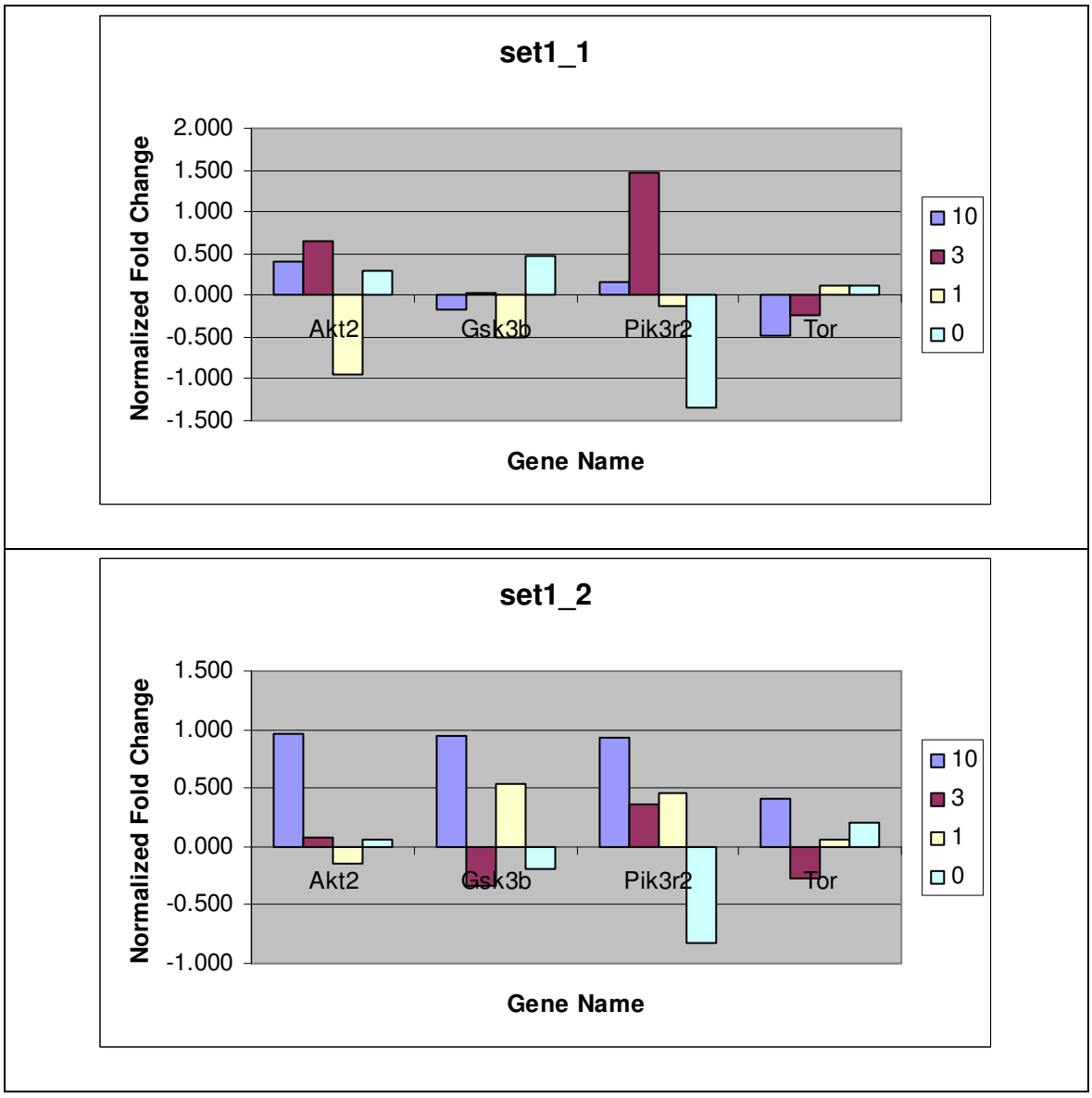

Figure 4.18. Log expression changes of akt2, gsk3b, pi3k, and tor genes with regard to mipep; calibrator was the average threshold cycle values of 10-0% expression values.

CHAPTER V: DISCUSSION AND FUTURE PERSPECTIVES

5.1. Bioinformatics Analysis of Alternative Splicing of a Conserved Alternative Exon (CAE) of Robo2

In the present study, primarily the expression of Robo2 along with those of several members of PI3K/AKT/TOR pathway were examined in zebrafish larvae and adult tissues. In doing so, alternative forms of Robo2 was assessed in zebrafish. Bioinformatics analyses suggested that Robo2 gene structure might allow for alternative splicing events as predicted by the GeneScan findings. One of these potentially alternatively spliced exons, named CAE, was found to be highly conserved among different species from zebrafish to humans. The high sequence homology and preserved reading frame between the orthologous sequences of CAE suggested that this sequence was functionally important and conserved. However, it is likely that CAE could be incorporated in multiple robo2 isoforms other than the ones specified in this study since a recent study identified alternatively spliced forms of human and mouse Robo2 that differed in their 5' as well as 3' exon usage (Yue et al., 2006).

One evolutionarily plausible hypothesis to explain the differential incorporation of CAE into the functional protein structure of robo family members could involve the exclusion of CAE in robo3 and tissue-specific inclusion of CAE in robo2. On the other hand, robo1 and robo4 could contain CAE either constitutively or alternatively, although no EST without CAE has been reported yet. It is possible that the incorporation of the CAE into robo1 and robo4 protein structure might be crucial for their function, whereas its exclusion could be dispensible or only condition-specifically advantageous, thus leading to functional divergence in other robo paralogs. The alternative usage of CAE in robo paralogs accordingly warrants future functional studies.

5.2. Differential Expression of Robo2 Isoforms in Zebrafish and Rats

The two isoforms, robo2_tv1 and robo2_tv2, identified in the present study differed in their use of CAE, located in the intracellular part of the protein. The extracellular Ig domains allow the binding of slit leucine-rich regions, whereas the intracellular portion of robo2 relays the signal (Chen et al. 2001; Battye et al. 2001; Nguyen Ba-Charvet et al. 2001; Liu et al. 2004). It is interesting that while the extracellular domain of robo2 is evolutionarily conserved, the intracellular domain has been shown to be divergent (Lee et al. 2001). The high-level expression of the robo2_tv2 and the scanty expression of the robo2_tv1 in non-neuronal tissues suggest the possible compartmentalization of the cell migratory and axon guidance roles in the developing animal. Further studies are needed to assess whether robo2 isoforms that contain CAE could have a role beyond regulating the cytoskeleton; they perhaps act as transcriptional factors (Couch et al. 2004) regulating the extent and timing of the molecular events leading to tissue morphogenesis.

In rats, the expression of the robo2_tv1 isoform without CAE was found predominantly in the brain similar to that of zebrafish. Several distinguishing features between zebrafish and rats were also obvious with regards to the transcription of CAE. The expression of CAE seemed to be more ubiquitous in rats and, thus, was found in both the neuronal and non-neuronal tissues unlike in zebrafish. Moreover, zebrafish heart contained very little of either isoforms, if any, whereas both were detectable in rats. The expression levels of robo2_tv1 in brain and testis were relatively high compared to other tissues; this expression profile was in accord with the findings of a recent study on alternative splicing capacities of human tissues (Yeo et al. 2004). It has been reported that the brain and testis have the highest levels of exon-skipping events while the ovary is one of the tissues likely to have multiple isoforms simultaneously. A previous study had reported the absence of robo2 in human adult tissues including liver (Nagase et al. 2000). If we assume high similarity between the expression profiles of rat and human; the observed difference could be because of the detection of different isoforms of the same gene. In addition to this, the expression pattern differences observed between rat and zebrafish were particularly interesting; however, the adult robo2 isoform expression in

non-neural tissues might rather be regulated at the protein level whereas the relative amount of the described robo2 isoforms in zebrafish could be transcriptionally and/or translationally regulated.

In summary, an alternative splicing event in a highly conserved predicted exon (CAE) in Robo2 genes of zebrafish and rat was identified and experimentally verified (Figures 4.7 and 4.8). CAE of zebrafish was transcribed in most of the non-neuronal tissues while it was either absent or expressed at a very low level in the brain, eye, and heart. Furthermore, the isoform-specific expression of Robo2 appeared to be tightly controlled during development such that zebrafish larvae exhibited an expressional induction of robo2_tv1 and robo2_tv2 at around the mid-larval stages. These findings might implicate robo2_tv2 in a role in tissue morphogenesis, during which cell growth/migration is temporally and spatially regulated. There is unearthed evidence indicating that tissue-type-dependent and, in some cases, neuronal non-neuronal tissue-distinct expression profiles result from alternative splicing events (Fukuda 2003; Shen et al. 2002; Jin et al. 2002; Rahman et al. 2002; Ramming et al. 2000; Hu et al. 1999). Some robo family members have previously been shown to exhibit alternatively spliced isoforms leading to functional divergence within Robo paralogs (Clark et al. 2002; Challa et al. 2005; Camurri et al. 2005). The differential expression of Robo2 isoforms in neuronal and non-neuronal tissues could similarly become a source of variation in the function of Robo2, possibly directed by different regulatory processes. Our findings strongly point to the existence of multiple Robo2 proteins; thus, it is critical to identify which form is involved in a specific developmental process or event in pathogenesis (Latil et al. 2003).

5.3. Bioinformatics Analyses of Robo2 and PI3K/AKT/TOR pathway

Meta-gene dataset analyses provided a list of genes that could increase our understanding in the coexpressed neighbors of Robo2. These findings suggested that TOR signaling is tightly correlated with the species-wise conserved patterns of gene expression as demonstrated by Stuart et al. (2003). Robo2 gene was found to be

coexpressed with FRAP1 (mTOR). Furthermore, the neighbors of FRAP1 included HIPK (Homeodomain-interacting Protein Kinase) isoforms as well as MAP3K5 (mitogen-activated protein kinase kinase kinase 5), which previous studies have identified its role in rapamycin mediated apoptosis in rhabdosarcoma cell lines (Huang et al. 2004; Song and Lee, 2003). These results suggested that Tor and Robo2 could be closely linked in their regulation as well as their response to inhibition by rapamycin or nutrient deprivation.

Another source of coexpression information between Robo2 and PI3K/AKT/TOR pathway came from the results of pathway-focused clustering of the Mathavan et al. (2005) dataset. Interestingly, several TOR signaling pathway members' expression patterns closely matched that of Robo2. On the other hand, PI3K signaling downstream components exhibited a reverse pattern with that of Robo2. For example, Rheb and Robo2 were developmentally coregulated. Rheb is one of the main regulators of TOR pathway such that, insulin-induced activity of Pik3 results in the activation of Rheb, a regulatory protein downstream of Tsc2 with GTPase activity (Saucedo et al. 2003; Stocker et al. 2003; Castro et al. 2003; Garamiet al. 2003; Inoki et al. 2003). Mathavan et al. data analysis also suggested that Rsks (Ribosomal protein S6 kinases) were downregulated. Recent studies have shown that Rsk1 (p90 S6 kinase) phosphorylation of Tsc2 leads to activation of mTOR (Roux et al. 2004). However, long-term insulin-Pik3 pathway activation is negatively regulated by a decrease in Irs-1 protein and activity levels; and rapamycin prevents this from happening (Hartley and Cooperm 2002; Haruta et al. 2000). Another gene corregulated with Robo2 was found to be PP2A based on our bioinformatics analyses. PP2A inhibition has been shown to be responsible for the change in IRS-1 mobility and constitutive serine/threonine phosphorylation (Hartley and Cooper, 2002). Several kinases phosphorylate Irs-1 at the serine/threonine residues, including, Gsk3β, Ikk1,2, Pkc, and S6k (see Harrington et al., 2005 for a complete list), S6k1 and S6k2 seem to be downstream effectors of mTOR in regulation of the Irs-1 (Harrington et al. 2004). Furthermore, the implication of Wnt signaling in Robo2 function in zebrafish is valuable since wnt signaling is known to be involved both in transcriptional regulation in carcinogenesis as well as actin cytoskeletal regulation.

5.4. Expression Analysis of Robo2, Pik3r2, Akt2, Tor, and Gsk3b in 48 hpf Embryos in Response to Rapamycin and in ZF4 Cells under Serum Deprivation

The findings of this study suggested that there might be a specific pattern of expression when embryos were exposed to rapamycin. This included a potential increase in robo2, tor, and gsk3b, yet a decline in the expression level of pi3kr2 and to a lesser degree in akt2. It can be suggested that robo2 might increase in response to rapamycin-induced growth arrest and/or apoptosis. These results suggested that PI3K and AKT2 signaling might be regulated at the transcriptional level, possibly allowing for reduced levels of Pik3r2 and Akt2 proteins under the studied conditions. These implicate Robo2 with a potential role in growth inhibition together with Gsk3b. Furthermore, since there are two different TOR complexes, the amount of available TOR might play a role in the activity profile of the TOR protein. Similarly, serum starvation experiments also suggested that Pik3r2 expression was the most affected in a negative manner. It is important to note that there has been no information about the expression patterns of zebrafish Pik3r2, Gsk3b, Akt2, and Tor in the literature; and the present study suggest that these genes might be regulated at the transcriptional level and thus warrants further study.

The expression data obtained from the present study rely on real-time RT-PCR experiments. Nevertheless, this analysis is prone to error for the detection of fold differences less than 2-fold when performing experiments. Since the rapamycin experiment was performed on three different sets of embryos, which were obtained from different strains, contained a high degree of variability as was reflected in the mRNA levels (Table 4.7). However, it must be noted that for a complete description of expression level changes of the interested genes under rapamycin treatment, it is necessary to perform replications for different strains for statistical inference.

Overall, this study provided a link between cell migratory and cell growth pathways, as the correlation between the mRNA expression levels of robo2, a gene with a well-known cell migratory activity, and the members of PI3K/AKT/TOR pathway, which is an important regulator of cell growth, could be shown computationally and to a certain degree, experimentally. Future studies are needed to extract and confirm the compendium of the conditions under which robo2 is modulated transcriptionally. Moreover, whether this transcriptional regulation is reflected at the protein level also needs to be assessed.

5.5. Future Perspectives

Our findings implicated Wnt signaling as well as PI3K/AKT/MAPK signaling as pathways that might be coregulated together with Robo2 expression. Therefore, future studies will focus on verification of the identified genes (Table 4.5) from the Mathavan et al., (2005) dataset using experiments in which cellular growth has been regulated (e.g., rapamycin treatment, stress conditions such as starvation and heat shock).

In order to increase the reliability and repeatibility of the future real-time RT-PCR analyses, other reference genes in addition to mipep are planned to be used. This will decrease the error associated with estimation of the total RNA levels to normalize the expression levels from different samples. Furthermore, rapamycin experiments will be performed with AB/Tub strain indepedently to increase the sample size thus to confirm the rapamycin experiment results obtained in this study. Serum starvation experiments also need to be repeated for making the statistical analysis possible. These future studies will allow us to assess whether Tor, Gsk3b, Pik3r2, and Akt are coexpressed under different cellular conditions thus are transcriptionally regulated in addition to their well known translational control mechanisms (e.g., phosphorylation and cellular translocation).

For rapamycin and serum starvation experiments we couldn't analyze the expression patterns of the two isoforms independently because the primer set produced more than one product and the alternative-isoform specific primers yielded dimers more

than expected. Therefore, other sets of primers should be designed for the quantitative analysis of different isoforms since real-time studies require dimer-free single amplicons for accurate measurement of expression. Once, the two isoforms could be identified independently then it would be possible to assess whether any of the isoforms were specific to cellular conditions such as growth arrest or cellular transformation.

CHAPTER VI: REFERENCES

Airaksinen S, Jokilehto T, Rabergh CM, Nikinmaa M. (2003) Heat- and cold-inducible regulation of HSP70 expression in zebrafish ZF4 cells. *Comp Biochem Physiol B Biochem Mol Biol.* **136(2)**:275-82.

Altmann SM, Mellon MT, Johnson MC, Paw BH, Trede NS, Zon LI, Kim CH. (2004) Cloning and characterization of an Mx gene and its corresponding promoter from the zebrafish, Danio rerio. *Developmental & Comparative Immunology*, **28(4)**: 295-306.

Altomare DA, You H, Xiao GH, Ramos-Nino ME, Skele KL, De Rienzo A, Jhanwar SC, Mossman BT, Kane AB, Testa JR. (2005) Human and mouse mesotheliomas exhibit elevated AKT/PKB activity, which can be targeted pharmacologically to inhibit tumor cell growth. *Oncogene.* **24(40)**:6080-9.

Anselmo MA, Dalvin S, Prodhan P, Komatsuzaki K, Aidlen JT, Schnitzer JJ, Wu JY, Kinane TB (2003) Slit and robo: expression patterns in lung development. *Gene Expr Patterns.* **3(1)**:13-9

Bagri A, Marin O, Plump AS, Mak J, Pleasure SJ, Rubenstein JL, Tessier-Lavigne M (2002) Slit proteins prevent midline crossing and determine the dorsoventral position of major axonal pathways in the mammalian forebrain. *Neuron.* **33(2)**:233-48

Basile JR, Castilho RM, Williams VP, Gutkind JS. (2006) Semaphorin 4D provides a link between axon guidance processes and tumor-induced angiogenesis. *Proc Natl Acad Sci U S A.*

Battye R, Stevens A, Perry RL, Jacobs JR (2001) Repellent signaling by Slit requires the leucine-rich repeats. *J Neurosci.* **21**:4290-4298

Bedell VM, Yeo SY, Park KW, Chung J, Seth P, Shivalingappa V, Zhao J, Obara T, Sukhatme VP, Drummond IA, Li DY, Ramchandran R. (2005) roundabout4 is essential for angiogenesis in vivo. *Proc Natl Acad Sci U S A.* **102(18)**:6373-8

Beugnet, A., Wang, X., and Proud, C.G. (2003) Target of rapamycin (TOR)-signaling and RAIP motifs play distinct roles in the mammalian TOR-dependent phosphorylation of initiation factor 4E-binding protein 1. *J. Biol. Chem.* **278**: 40717-40722.

Bieche I, Lerebours F, Tozlu S, Espie M, Marty M, Lidereau R. (2004) Molecular profiling of inflammatory breast cancer: identification of a poor-prognosis gene expression signature.
Clin Cancer Res. **10(20)**:6789-95.

Brummendorf T, Lemmon V (2001) Immunoglobulin superfamily receptors: cis-interactions, intracellular adapters and alternative splicing regulate adhesion. *Curr Opin Cell Biol.* **13(5)**:611-8.

Brunn GJ, Williams J, Sabers C, Wiederrecht G, Lawrence JJC, Abraham RT. (1996) Direct inhibition of the signaling functions of the mammalian target of rapamycin by the phosphoinositide 3-kinase inhibitors, wortmannin and LY294002. *EMBO J.* **15**: 5256-5267.

Cao X, Kambe F, Moeller LC, Refetoff S, Seo H. (2005) Thyroid hormone induces rapid activation of Akt/protein kinase B-mammalian target of rapamycin-p70S6K cascade through phosphatidylinositol 3-kinase in human fibroblasts. *Mol Endocrinol.* **19(1)**:102-12.

Calne RY, Collier DS, Lim S, Pollard SG, Samaan A, White DJ, Thiru S. (1989) Rapamycin for immunosuppresion in organ allografting. *Lancet*. **2**:227.

Carpenter CL, Duckworth BC, Auger KR, Cohen B, Schaffhausen BS, Cantley LC. (1990) Purification and characterization of phosphoinositide 3-kinase from rat liver. *J Biol Chem.* **265(32)**:19704-11.

Castro AF, Rebhun JF, Clark GJ, Quilliam LA. (2003) Rheb binds tuberous sclerosis complex 2 (TSC2) and promotes S6 kinase activation in a rapamycin- and farnesylation-dependent manner. *J. Biol. Chem.* **278**: 32493-32496.

Chan KM, Ku LL, Chan PC, Cheuk WK. (2006) Metallothionein gene expression in zebrafish embryo-larvae and ZFL cell-line exposed to heavy metal ions. *Mar Environ Res.*

Cheatham B, Vlahos CJ, Cheatham L, Wang L, Blenis J, Kahn CR. (1994) Phosphatidylinositol 3-kinase activation is required for insulin stimulation of pp70 S6 kinase, DNA synthesis, and glucose transporter translocation. *Mol. Cell. Biol.* **14**: 4902-4911.

Chedotal A, Kerjan G, Moreau-Fauvarque C. (2005) The brain within the tumor: new roles for axon guidance molecules in cancers. *Cell Death Differ.* **12(8)**:1044-56.

Chen JH, Wen L, Dupuis S, Wu JY, Rao Y. (2001) The N-terminal leucine rich regions in Slit are sufficient to repel olfactory bulb axons and subventricular zone neurons. *J Neurosci.* **21**:1548-1556.

Chen PY, Manninga H, Slanchev K, Chien M, Russo JJ, Ju J, Sheridan R, John B, Marks DS, Gaidatzis D, Sander C, Zavolan M, Tuschl T. (2005) The developmental miRNA profiles of zebrafish as determined by small RNA cloning. *Genes Dev.* **19(11)**:1288-93.

Chilton JK. (2006) Molecular mechanisms of axon guidance, *Developmental Biology* **292(1)**: 13-24.

Choi KM, McMahon LP, Lawrence JJC. (2003) Two motifs in the translational repressor PHAS-I required for efficient phosphorylation by mammalian target of rapamycin and for recognition by raptor. *J. Biol. Chem.* **278**: 19667-19673.

Chung J, Grammer TC, Lemon KP, Kazlauskas A, Blenis J. (1994) PDGF- and insulin-dependent pp70S6k activation mediated by phosphatidylinositol-3-OH kinase. *Nature* **370**: 71-75.

Clark K, Hammond E, Rabbitts P. (2002) Temporal and spatial expression of two isoforms of the Dutt1/Robo1 gene in mouse development. *FEBS Letters* **523**:12-16

Couch JA, Chen J, Rieff HI, Uri EM, Condron BG. (2004) Robo2 and Robo3 interact with Eagle to regulate serotonergic neuron differentiation. *Development* **131**:997-1006.

Dann SG, Thomas G. (2006) The amino acid sensitive TOR pathway from yeast to mammals. *FEBS Lett.* **580(12)**:2821-9.

Dalkic E, Kuscu C, Sucularli C, Aydin IT, Akcali KC, Konu O. (2006) Alternatively spliced Robo2 isoforms in zebrafish and rat. *Dev Genes Evol.* [Epub ahead of print]

Dennis PB, Jaeschke A, Saitoh M, Fowler B, Kozma SC, Thomas G. (2001) Mammalian TOR: A homeostatic ATP sensor. *Science* **294**: 1102-1105

Di Como, C.J. and Arndt, K.T. (1996) Nutrients, via the Tor proteins, stimulate the association of Tap42 with type 2A phosphatases. *Genes & Dev.* **10**: 1904-1916

Douros J, Suffness M. (1981) New antitumor substances of natural orgin. *Cancer Treat Rev*. **8**:63-87.

Driever W, Rangini Z. (1993) Characterization of a cell line derived from zebrafish (Brachydanio rerio) embryos. *In Vitro Cell Dev Biol Anim***. 29A(9)**:749-54.

Feng Z, Zhang H, Levine AJ, Jin S. (2005) The coordinate regulation of the p53 and mTOR pathways in cells. *Proc Natl Acad Sci U S A* **102(23)**:8204-9.

Fukuda M (2003) Molecular cloning and characterization of human, rat, and mouse synaptotagmin XV. *Biochem Biophys Res Commun.* **306(1)**:64-71.

Fricke C, Lee JS, Geiger-Rudolph S, Bonhoeffer F, Chien CB (2001) Astray, a zebrafish Roundabout homolog required for retinal axon guidance. *Science* **292**:507-510.

Gao, X. and Pan, D. (2001) TSC1 and TSC2 tumor suppressors antagonize insulin signaling in cell growth. *Genes & Dev.* **15**: 1383-1392.

Gao, X., Zhang, Y., Arrazola, P., Hino, O., Kobayashi, T., Yeung, R.S., Ru, B., and Pan, D. (2002) Tsc tumour suppressor proteins antagonize amino-acid-TOR signalling. *Nat. Cell. Biol.* **4**: 699-704.

Garami A, Zwartkruis FJ, Nobukuni T, Joaquin M, Roccio M, Stocker H, Kozma SC, Hafen E, Bos JL, Thomas G. (2003) Insulin activation of Rheb, a mediator of mTOR/S6K/4E-BP signaling, is inhibited by TSC1 and 2. *Mol. Cell* **11**: 1457-1466.

Garg R, Geng CD, Miller JL, Callens S, Tang X, Appel B, Xu B. (2004) Molecular cloning and characterization of the catalytic domain of zebrafish homologue of the ataxia-telangiectasia mutated gene. *Mol Cancer Res.* **2(6)**:348-53.

Gingras AC, Kennedy SG, O'Leary MA, Sonenberg N, Hay N. (1998) 4E-BP1, a repressor of mRNA translation, is phosphorylated and inactivated by the Akt(PKB) signaling pathway. *Genes & Dev.* **12**: 502-513.

Goncharova EA, Goncharov DA, Eszterhas A, Hunter DS, Glassberg MK, Yeung RS, Walker CL, Noonan D, Kwiatkowski DJ, Chou MM (2002) Tuberin regulates p70 S6 kinase activation and ribosomal protein S6 phosphorylation. A role for the TSC2 tumor suppressor gene in pulmonary lymphangioleiomyomatosis (LAM). *J. Biol. Chem.* **277**: 30958-30967.

Greenberg JM, Thompson FY, Brooks SK, Shannon JM, Akeson AL (2004) Slit and robo expression in the developing mouse lung. *Dev Dyn.* **230(2)**:350-60

Grieshammer U, Le M, Plump AS, Wang F, Tessier-Lavigne M, Martin GR (2004) SLIT2 mediated ROBO2 signaling restricts kidney induction to a single site. *Dev. Cell* **6**:709-717

Grone J, Doebler O, Loddenkemper C, Hotz B, Buhr HJ, Bhargava S. (2006) Robo1/Robo4: Differential expression of angiogenic markers in colorectal cancer. *Oncol Rep.* **15(6)**:1437-43.

Hardie DG, Carling D, Carlson M. (1998) The AMP-activated/SNF1 protein kinase subfamily: metabolic sensors of the eukaryotic cell? *Annu Rev Biochem.* **67**:821-55.

Harrington L.S. (2004) The TSC1-2 tumor suppressor controls insulin-PI3K signaling via regulation of IRS proteins. *J. Cell Biol.* **166**, 213–223.

Hartley D and Cooper GM. (2002) Role of mTOR in the degradation of IRS-1: regulation of PP2A activity. *J. Cell. Biochem.* **85**, 304–314.

Haruta T, Uno T, Kawahara J, Takano A, Egawa K, Sharma PM, Olefsky JM, Kobayashi M. (2000) A rapamycin-sensitive pathway downregulates insulin signaling via phosphorylation and proteasomal degradation of insulin receptor substrate-1. *Mol. Endocrinol.* **14(6)**: 783–794.

Hay N and Sonenberg N. (2004) Upstream and downstream of mTOR. *Genes Dev.* **18**: 1926-1945.

Heitman J, Movva NR and Hall MN. (1991) Targets for cell cycle arrest by the immunosuppressant rapamycin in yeast. *Science* **253**: 905–909.

Hetman M, Xia Z. (2000) Signaling pathways mediating anti-apoptotic action of neurotrophins. *Acta Neurobiol Exp (Wars).* **60(4)**:531-45.

Hu Q, Hearn MG, Jin LW, Bressler SL, Martin GM (1999) Alternatively spliced isoforms of FE65 serve as neuron-specific and non-neuronal markers. *J Neurosci Res.* **58(5)**:632-40

Huang S, Houghton PJ. (2002) Mechanisms of resistance to rapamycins. *Drug Resistance Updates*. **4**:378-391.

Huang S, Shu L, Easton J, Harwood FC, Germain GS, Ichijo H, Houghton PJ. (2004) Inhibition of mammalian target of rapamycin activates apoptosis signal-regulating kinase 1 signaling by suppressing protein phosphatase 5 activity. *J Biol Chem.* **279(35)**:36490-6.

Huminiecki L, Gorn M, Suchting S, Poulsom R, Bicknell R. (2002) Magic roundabout is a new member of the roundabout receptor family that is endothelial specific and expressed at sites of active angiogenesis. *Genomics.* **79(4)**:547-52.

Inoki K, Li Y, Zhu T, Wu J, Guan KL. (2002) TSC2 is phosphorylated and inhibited by Akt and suppresses mTOR signalling. *Nat. Cell. Biol.* **4**: 648-657.

Inoki K, Li Y, Xu T, Guan KL. (2003a). Rheb GTPase is a direct target of TSC2 GAP activity and regulates mTOR signaling. *Genes & Dev.* **17**: 1829-1834

Inoki K, Zhu T, Guan KL. (2003b). TSC2 mediates cellular energy response to control cell growth and survival. *Cell* **115**: 577-590.

Irie HY, Pearline RV, Grueneberg D, Hsia M, Ravichandran P, Kothari N, Natesan S, Brugge JS. (2005) Distinct roles of Akt1 and Akt2 in regulating cell migration and epithelial-mesenchymal transition. *J Cell Biol.* **171(6)**:1023-34.

Inukai K, Funaki M, Anai M, Ogihara T, Katagiri H, Fukushima Y, Sakoda H, Onishi Y, Ono H, Fujishiro M, Abe M, Oka Y, Kikuchi M, Asano T. (2001) Five isoforms of the phosphatidylinositol 3-kinase regulatory subunit exhibit different associations with receptor tyrosine kinases and their tyrosine phosphorylations. *FEBS Lett.* **490(1-2)**:32-8.

Ito H, Funahashi S, Yamauchi N, Shibahara J, Midorikawa Y, Kawai S, Kinoshita Y, Watanabe A, Hippo Y, Ohtomo T, Iwanari H, Nakajima A, Makuuchi M, Fukayama M, Hirata Y, Hamakubo T, Kodama T, Tsuchiya M, Aburatani H. (2006) Identification of ROBO1 as a novel hepatocellular carcinoma antigen and a potential therapeutic and diagnostic target. *Clin Cancer Res.***12(11 Pt 1)**:3257-64.

Izuishi K, Kato K, Ogura T, Kinoshita T, Esumi H. (2000) Remarkable tolerance of tumor cells to nutrient deprivation: possible new biochemical target for cancer therapy. *Cancer Res.* **60(21)**:6201-7.

Jaeschke A, Hartkamp J, Saitoh M, Roworth W, Nobukuni T, Hodges A, Sampson J, Thomas G, Lamb R. (2002) Tuberous sclerosis complex tumor suppressor-mediated S6 kinase inhibition by phosphatidylinositide-3-OH kinase is mTOR independent. *J. Cell. Biol.* **159**: 217-224.

Jin M, Tanaka S, Sekino Y, Ren Y, Yamazaki H, Kawai-Hirai R, Kojima N, Shirao T (2002) A novel, brain-specific mouse drebrin: cDNA cloning, chromosomal mapping, genomic structure, expression, and functional characterization. *Genomics* **79(5)**:686-92

Kemp BE, Mitchelhill KI, Stapleton D, Michell BJ, Chen ZP, Witters LA. (1999) Dealing with energy demand: The AMP-activated protein kinase. *Trends Biochem. Sci.* **24**: 22-25.

Kidd T, Brose K, Mitchell KJ, Fetter RD, Tessier-Lavigne M, Goodman CS, Tear G (1998) Roundabout controls axon crossing of the CNS midline and defines a novel subfamily of evolutionarily conserved guidance receptors. *Cell* **92**:205-215

Kidd T, Bland KS, Goodman CS (1999) Slit is the midline repellent for the Robo receptor in Drosophila. *Cell* **96**:785-794

Kimmel CB, Ballard WW, Kimmel SR, Ullmann B, Schilling TF. (1995). *Developmental Dynamics*. **203**, 253.

Kim DH, Sarbassov DD, Ali SM., Latek RR, Guntur KV, Erdjument-Bromage H, Tempst P, Sabatini DM. (2003) GBL, a positive regulator of the rapamycin-sensitive pathway required for the nutrient-sensitive interaction between raptor and mTOR. *Mol. Cell* **11**: 895-904

Kimura N, Tokunaga C, Dalal S, Richardson C, Yoshino K, Hara K, Kemp BE, Witters LA, Mimura O, Yonezawa K. (2003) A possible linkage between AMP-activated protein kinase (AMPK) and mammalian target of rapamycin (mTOR) signalling pathway. *Genes Cells* **8**: 65-79.

Kuzman JA, Gerdes AM, Kobayashi S, Liang Q. (2005) Thyroid hormone activates Akt and prevents serum starvation-induced cell death in neonatal rat cardiomyocytes. *J Mol Cell Cardiol.* **39(5)**:841-4.

Kwiatkowski DJ, Zhang H, Bandura JL, Heiberger KM, Glogauer M, el-Hashemite N, Onda H. (2002) A mouse model of TSC1 reveals sex-dependent lethality from liver hemangiomas, and up-regulation of p70S6 kinase activity in Tsc1 null cells. *Hum. Mol. Genet.* **11**: 525-534.

Leicht M, Marx G, Karbach D, Gekle M, Kohler T, Zimmer HG. (2003) Mechanism of cell death of rat cardiac fibroblasts induced by serum depletion.
Mol Cell Biochem. 2**51(1-2)**:119-26.

Lam SH, Gong Z. (2006) Modeling liver cancer using zebrafish: a comparative oncogenomics approach. *Cell Cycle.* **5(6)**:573-7.

Lam SH, Wu YL, Vega VB, Miller LD, Spitsbergen J, Tong Y, Zhan H, Govindarajan KR, Lee S, Mathavan S, Murthy KR, Buhler DR, Liu ET, Gong Z. (2006) Conservation

of gene expression signatures between zebrafish and human liver tumors and tumor progression. *Nat Biotechnol.* **24(1)**:73-5.

Latil A, Chene L, Cochant-Priollet B, Mangin P, Fournier G, Berthon P, Cussenot O. (2003) Quantification of expression of netrins, slits and their receptors in human prostate tumors. *Int J Cancer.* **103(3)**:306-15.

Lee JS, Ray R, Chien CB (2001) Cloning and expression of three zebrafish Roundabout homologs suggest roles in axon guidance and cell migration. *Dev. Dyn.* **221**:216-230.

Lizcano JM, Alrubaie S, Kieloch A, Deak M, Leevers SJ, Alessi DR. (2003) Insulin-induced *Drosophila* S6 kinase activation requires phosphoinositide 3-kinase and protein kinase B. *Biochem. J.* **374**: 297-306.

Liu Z, Patel K, Schmidt H, Andrews W, Pini A, Sundaresan V (2004) Extracellular Ig domains 1 and 2 of Robo are important for ligand (Slit) binding. *Mol Cell Neurosci.* **26(2)**:232-40.

Long H, Sabatier C, Ma L, Plump A, Yuan W, Ornitz DM, Tamada A, Murakami F, Goodman CS, Tessier-Lavigne M. (2004) Conserved roles for Slit and Robo proteins in midline commissural axon guidance. *Neuron* **42(2)**:213-23.

Manning BD, Tee AR, Logsdon MN, Blenis J, Cantley LC. (2002) Identification of the tuberous sclerosis complex-2 tumor suppressor gene product tuberin as a target of the phosphoinositide 3-kinase/akt pathway. *Mol. Cell* **10**: 151-162.

Marillat V, Cases O, Nguyen-Ba-Charvet KT, Tessier-Lavigne M, Sotelo C, Chedotal A (2002) Spatiotemporal expression patterns of slit and robo genes in the rat brain. *J Comp Neurol.* **442(2)**:130-55.

Martin DE and Hall MN. (2005) The expanding TOR signaling network. *Current Opinion in Cell Biology*. **17(2)**: 158-166.

Matsumoto S, Bandyopadhyay A, Kwiatkowski DJ, Maitra U, Matsumoto T. (2002) Role of the Tsc1-Tsc2 complex in signaling and transport across the cell membrane in the fission yeast *Schizosaccharomyces pombe*. *Genetics* **161**: 1053-1063.

McGonnell IM, Fowkes RC. Fishing for gene function - endocrine modelling in the zebrafish. (2006) *J Endocrinol.* **189(3)**:425-39.

Mendez R, Myers JMG, White MF, Rhoads RE. (1996) Stimulation of protein synthesis, eukaryotic translation initiation factor 4E phosphorylation, and PHAS-I phosphorylation by insulin requires insulin receptor substrate 1 and phosphatidylinositol 3-kinase. *Mol. Cell. Biol.* **16**: 2857-2864.

Miron M, Lasko P, Sonenberg N. 2003. Signaling from Akt to FRAP/TOR targets both 4E-BP and S6K in *Drosophila melanogaster*. *Mol. Cell. Biol.* **23**: 9117-9126.

Nagase T, Kikuno R, Nakayama M, Hirosawa M, Ohara O. (2000) Prediction of the coding sequences of unidentified human genes. XVIII. The complete sequences of 100 new cDNA clones from brain which code for large proteins in vitro. *DNA Res.* **7**: 273-281.

Narayan G, Goparaju C, Arias-Pulido H, Kaufmann AM, Schneider A, Durst M, Mansukhani M, Pothuri B, Murty VV. (2006) Promoter hypermethylation-mediated inactivation of multiple Slit-Robo pathway genes in cervical cancer progression. *Mol Cancer.* **5(1)**:16.

Neshat MS, Mellinghoff IK, Tran C, Stiles B, Thomas G, Petersen R, Frost P, Gibbons, JJ, Wu H, Sawyers CL. 2001. Enhanced sensitivity of PTEN-deficient tumors to inhibition of FRAP/mTOR. *Proc. Natl. Acad. Sci.* **98**: 10314-10319.

Nguyen Ba-Charvet KT, Brose K, Ma L, Wang KH, Marillat V, Sotelo C, Tessier-Lavigne M, Chedotal A (2001) Diversity and specificity of actions of Slit2 proteolytic fragments in axon guidance. *J Neurosci.* **21**:4281-4289.

Nusslein-Volhard C, Wieschaus E, Kluding H (1984) Mutations affecting the pattern of the larval cuticle in Drosophila Melanogaster. I.Zygotic loci on the second chromosome. *Roux's Arch Dev Biol.* **193**:267-282.

Patel S, Doble B, Woodgett JR. (2004) Glycogen synthase kinase-3 in insulin and Wnt signalling: a double-edged sword? *Biochem Soc Trans.* **32(Pt 5)**:803-8.

Peterson RT, Desai BN, Hardwick JS, Schreiber SL. (1999) Protein phosphatase 2A interacts with the 70-kDa S6 kinase and is activated by inhibition of FKBP12-rapamycin associated protein. *Proc. Natl. Acad. Sci.* **96**: 4438-4442.

Pfaffl MW. (2001) A new mathematical model for relative quantification in real-time RT-PCR. *Nucleic Acids Res.* **29(9)**:e45.

Piper M, Georgas K, Yamada T, Little M (2000) Expression of the vertebrate Slit gene family and their putative receptors, the Robo genes, in the developing murine kidney. *Mech Dev.* **94(1-2)**:213-7.

Podsypanina K, Lee RT, Politis C, Hennessy I, Crane A, Puc J, Neshat M, Wang H, Yang L, Gibbons J, Frost P, Dreisbach V, Blenis J, Gaciong Z, Fisher P, Sawyers C, Hedrick-Ellenson L, Parsons R. (2001) An inhibitor of mTOR reduces neoplasia and normalizes p70/S6 kinase activity in Pten$^{+/-}$ mice. *Proc. Natl. Acad. Sci.* **98**: 10320-10325.

Potter CJ, Huang H, Xu T. (2001) *Drosophila* Tsc1 functions with Tsc2 to antagonize insulin signaling in regulating cell growth, cell proliferation, and organ size. *Cell* **105**: 357-368.

Rahman L, Bliskovski V, Reinhold W, Zajac-Kaye M (2002) Alternative splicing of brain-specific PTB defines a tissue-specific isoform pattern that predicts distinct functional roles. *Genomics* **80(3)**:245-9

Rajagopalan S, Vivancos V, Nicolas E, Dickson BJ (2000a) Selecting a longitudinal pathway: Robo receptors specify the lateral position of axons in the Drosophila CNS. *Cell* **103**:1033-1045

Rajagopalan S, Nicolas E, Vivancos V, Berger J, Dickson BJ (2000b) Crossing the midline: roles and regulation of Robo receptors. *Neuron* **28**:767-777

Ramming M, Kins S, Werner N, Hermann A, Betz H, Kirsch J (2000) Diversity and phylogeny of gephyrin: tissue-specific splice variants, gene structure, and sequence similarities to molybdenum cofactor-synthesizing and cytoskeleton-associated proteins. *Proc Natl Acad Sci USA*. **97(18):**10266-71

Risbud MV, Fertala J, Vresilovic EJ, Albert TJ, Shapiro IM. (2005) Nucleus pulposus cells upregulate PI3K/Akt and MEK/ERK signaling pathways under hypoxic conditions and resist apoptosis induced by serum withdrawal. *Spine.* 30(8):882-9.

Rothberg JM, Hartley DA, Walther Z, Artavanis-Tsakonas S (1988) Slit: an EGF-homologous locus of D.melanogaster involved in the development of the embryonic central nervous system. *Cell* **55**:1047-1059

Roux PP, Ballif BA, Anjum R, Gygi SP, Blenis J. (2004) Tumor-promoting phorbol esters and activated Ras inactivate the tuberous sclerosis tumor suppressor complex via p90 ribosomal S6 kinase. *Proc. Natl. Acad. Sci. U. S. A.* **101(37)**: 13489–13494.

Saucedo LJ, Gao X, Chiarelli DA, Li L, Pan D, Edgar BA. (2003) Rheb promotes cell growth as a component of the insulin/TOR signalling network. *Nat. Cell. Biol.* **5**: 566-571.

Scanga SE, Ruel L, Binari RC, Snow B, Stambolic V, Bouchard D, Peters M, Calvieri B, Mak TW, Woodgett JR et al. (2000) The conserved PI3K/PTEN/Akt signaling pathway regulates both cell size and survival in *Drosophila*. *Oncogene* **19**: 3971-3977.

Schalm SS, Fingar DC, Sabatini DM, Blenis J. (2003) TOS motif-mediated raptor binding regulates 4E-BP1 multisite phosphorylation and function. *Curr. Biol.* 13: 797-806.

Seeger M, Tear G, Ferres-Marco D, Goodman CS (1993) Mutations affecting growth cone guidance in Drosophila: genes necessary for guidance toward or away from the midline. **Neuron 10**:409-426

Sehgal SN, Baker H, Vezina C. (1975) Rapamycin(AY-22,989), a new antifungal antibiotic. II. Fermentation, isolation and characterization. *J Antibiot(Tokyo)*. **28**:727-732.

Sehgal SN. Rapamune(RAPA, rapamycin, sirolimus):mechanism of action immunosuppresive effect results from blocade of signal transduction and inhibition of cell cycle progression. 1998 *Clin Biochem*. **31**:335-340.

Shah OJ, Wang Z, Hunter T. (2004) Inappropriate activation of the TSC/Rheb/mTOR/S6K cassette induces IRS1/2 depletion, insulin resistance, and cell survival deficiencies. *Curr. Biol.* **14(18)**, 1650–1656.

Shen H, Illges H, Reuter A, Stuermer CAO. (2002) Cloning, expression, and alternative splicing of neogenin1 in zebrafish. *Mechanisms of Development* **118:**219-223.

Simpson JH, Bland KS, Fetter RD, Goodman CS (2000a) Short-range and long-range guidance by Slit and its Robo receptors: a combinatorial code of Robo receptors controls lateral position. *Cell* **103**:1019-1032.

Simpson JH, Kidd T, Bland KS, Goodman CS (2000b) Short-range and long-range guidance by Slit and its Robo receptors: Robo and Robo2 play distinct roles in midline guidance. *Neuron* **28**:753-766.

Stocker H, Radimerski T, Schindelholz B, Wittwer F, Belawat P, Daram P, Breuer S, Thomas G, Hafen E. (2003) Rheb is an essential regulator of S6K in controlling cell growth in *Drosophila*. *Nat. Cell. Biol.* **5**: 559-565.

Streisinger G, Walker C, Dower N, Knauber D, Singer F. (1981) Production of clones of homozygous diploid zebra fish (Brachydanio rerio). *Nature* May **28**:291(5813):293-6.

Stuart JM, Segal E, Koller D, Kim SK. (2003) A Gene-Coexpression Network for Global Discovery of Conserved Genetic Moldules. *Science* **302**:249-255

Sundaresan V, Mambetisaeva E, Andrews W, Annan A, Knoll B, Tear G, Bannister L (2004) Dynamic expression patterns of Robo (Robo1 and Robo2) in the developing murine central nervous system. *J Comp Neurol.* **468(4)**:467-81.

Tapon, N., Ito, N., Dickson, B.J., Treisman, J.E., and Hariharan, I.K. (2001) The *Drosophila* tuberous sclerosis complex gene homologs restrict cell growth and cell proliferation. *Cell* **105**: 345-355.

Tee AR, Fingar DC, Manning BD, Kwiatkowski DJ, Cantley LC, Blenis, J. (2002) Tuberous sclerosis complex-1 and -2 gene products function together to inhibit mammalian target of rapamycin (mTOR)-mediated downstream signaling. *Proc. Natl. Acad. Sci.* **99**: 13571-13576.

Titus TA, Selvig DR, Qin B, Wilson C, Starks AM, Roe BA, Postlethwait JH. (2006) The Fanconi anemia gene network is conserved from zebrafish to human. *Gene*. **371(2)**:211-23.

Tresini M, Mawal-Dewan M, Cristofalo VJ, Sell C. (1998) A phosphatidylinositol 3-kinase inhibitor induces a senescent-like growth arrest in human diploid fibroblasts. *Cancer Res.* **58(1):**1-4.

Tsurutani J, West KA, Sayyah J, Gills JJ, Dennis PA. (2005) Inhibition of the phosphatidylinositol 3-kinase/Akt/mammalian target of rapamycin pathway but not the MEK/ERK pathway attenuates laminin-mediated small cell lung cancer cellular survival and resistance to imatinib mesylate or chemotherapy. *Cancer Res.* **65(18)**:8423-32.

van Slegtenhorst, M., Carr, E., Stoyanova, R., Kruger, W.D., and Henske, E.P. 2004. Tsc1+ and tsc2+ regulate arginine uptake and metabolism in *Schizosaccharomyces pombe*. *J. Biol. Chem.* **279**: 12706-12713.

Vargesson N, Luria V, Messina I, Erskine L, Laufer E (2001) Expression patterns of Slit and Robo family members during vertebrate limb development. *Mech Dev.* **106(1-2)**:175-80.

Verdu, J., Buratovich, M.A., Wilder, E.L., and Birnbaum, M.J. (1999) Cell-autonomous regulation of cell and organ growth in *Drosophila* by Akt/PKB. *Nat. Cell. Biol.* **1**: 500-506.

von Manteuffel, S.R., Gingras, A.C., Ming, X.F., Sonenberg, N., and Thomas, G. (1996) 4E-BP1 phosphorylation is mediated by the FRAP-p70s6k pathway and is independent of mitogen-activated protein kinase. *Proc. Natl. Acad. Sci.* **93**: 4076-4080.

Wang L, Wu Q, Qiu P, Mirza A, McGuirk M, Kirschmeier P, Greene JR, Wang Y, Pickett CB, Liu S. (2001) Analyses of p53 target genes in the human genome by bioinformatic and microarray approaches. *J Biol Chem.* **276(47)**:43604-10
Wang B, Xiao Y, Ding BB, Zhang N, Yuan X, Gui L, Qian KX, Duan S, Chen Z, Rao Y, Geng JG. (2003) Induction of tumor angiogenesis by Slit-Robo signaling and inhibition of cancer growth by blocking Robo activity. *Cancer Cell.* **4(1)**:19-29.

Wentworth JN, Buzzeo R, Pollenz RS. (2004) Functional characterization of aryl hydrocarbon receptor (zfAHR2) localization and degradation in zebrafish (Danio rerio). *Biochem Pharmacol* .**67(7):**1363-72.

Wong K, Park HT, Wu JY, Rao Y (2002) Slit proteins: molecular guidance cues for cells ranging from neurons to leukocytes. *Curr Opin Genet Dev.* **12(5)**:583-91

Woodgett JR. Recent advances in the protein kinase B signaling pathway *Current Opinion in Cell Biology* **(17:2):** 150-157

Yuan SSF, Cox LA, Dasika GK, Lee EYHP (1999) Cloning and functional studies of a novel gene aberrantly expressed in RB-deficient embryos. *Dev Biol.* **207(1):**62-75

Yuan W, Zhou L, Chen JH, Wu JY, Rao Y, Ornitz DM (1999) The mouse SLIT family: secreted ligands for ROBO expressed in patterns that suggest a role in morphogenesis and axon guidance. *Dev Biol.* **212(2):**290-306.

Yue Y, Grossmann B, Galetzka D, Zechner U, Haaf T. (2006) Isolation and differential expression of two isoforms of the ROBO2/Robo2 axon guidance receptor gene in humans and mice. *Genomics.* [Epub ahead of print]

Zhang H, Cicchetti G, Onda H, Koon HB, Asrican K, Bajraszewski N, Vazquez F, Carpenter CL, Kwiatkowski DJ. (2003) Loss of Tsc1/Tsc2 activates mTOR and disrupts PI3K–Akt signaling through downregulation of PDGFR. *J. Clin.Invest.* **112(8)**: 1223–1233.

Zhao H, Dupont J, Yakar S, Karas M, LeRoith D. (2004) PTEN inhibits cell proliferation and induces apoptosis by downregulating cell surface IGF-IR expression in prostate cancer cells *Oncogene.* **23(3)**:786-94.

APPENDIX

Threshold cycles for rapamycin Real-time RT-PCRs were listed below. For genes that had multiple values, mean values were given.

Experiment 1	**mipep**	**akt2**	**mipep**	**gsk3b**	**mipep**	**pi3k**	**mipep**	**tor**	**mipep**	**robo2**
control	22.35	21.45	22.35	22.25	22.35	22.1	22.35	24	22.3	23.1
rapamycin	22.05	21.9	22.05	21.7	22.05	22.5	22.05	23.9	22.4	22.05
Experiment 2	**mipep**	**akt2**	**mipep**	**gsk3b**	**mipep**	**pi3k**	**mipep**	**tor**	**mipep**	**robo2**
control	20.4	22.8	21.8	23.5	21.8	23.8	21.05	23.35	21.76	22.83
rapamycin	20.8	22.6	21.1	22.5	21.1	24.4	20.95	22.3	21.1	22.73
Experiment 3	mipep	**akt2**	mipep	**gsk3b**	mipep	**pi3k**	mipep	**tor**	mipep	**robo2**
control	29.25	29.05	30	31.65	29.25	27.95	28.05	30.65	28.8	29.45
rapamycin	26.45	26.55	26.8	27.3	26.45	25	25.65	28.1	26	25.9

Threshold cycles for serum starvation Real-time RT-PCRs were listed below.

Experiment 1_1	**Mipep**	**Akt2**	**Mipep**	**Gsk3b**	**Mipep**	**Pi3k**	**Mipep**	**Tor**	**Mipep**	**Robo2**
10% serum	25.8	23.5	25.8	26	25.8	27.4	25.8	24.8	25.8	32.2
3% serum	25.6	23.1	25.6	25.6	25.6	26	25.6	24.4	25.6	31.8
1% serum	27.6	26.3	27.6	28.1	27.6	29.2	27.6	25.8	27.6	31.8
0% serum	29.3	26.6	29.3	28.7	29.3	31.8	29.3	27.3	29.3	34.3
Experiment 1_2	**Mipep**	**Akt2**	**Mipep**	**Gsk3b**	**Mipep**	**Pi3k**	**Mipep**	**Tor**	**Mipep**	**Robo2**
10% serum	27.1	24.1	27.1	25.8	27.1	27.1	27.1	24.6	27.1	32.3
3% serum	25.9	23.9	25.9	26	25.9	26.6	25.9	24.2	25.9	31.1
1% serum	28.1	26	28.1	27.2	28.1	28.4	28.1	25.8	28.1	33
0% serum	30.2	27.6	30.2	30	30.2	31.4	30.2	27.5	30.2	32.4